

We are IntechOpen, the world's leading publisher of Open Access books Built by scientists, for scientists

5,800

Open access books available

142,000

International authors and editors

180M

Downloads

Our authors are among the

154

Countries delivered to

TOP 1%

most cited scientists

12.2%

Contributors from top 500 universities



WEB OF SCIENCE™

Selection of our books indexed in the Book Citation Index
in Web of Science™ Core Collection (BKCI)

Interested in publishing with us?
Contact book.department@intechopen.com

Numbers displayed above are based on latest data collected.
For more information visit www.intechopen.com



Recent Developments in All-Solid-State Micro-Supercapacitors Based on Two-Dimensional Materials

*Minu Mathew, Sithara Radhakrishnan
and Chandra Sekhar Rout*

Abstract

Owing to their unique features such as high surface area, rich electroactive sites, ultrathin thickness, excellent flexibility and mechanical stability and multiple surface functionalities enables outstanding electrochemical response which provides high energy and power density supercapacitors based on them. Also, the Van der Waals gap between layered 2D materials encourages the fast ion transport with shorter ion diffusion path. 2D materials such as MXenes, graphene, TMDs, and 2D metal–organic frame work, TMOs/TMHs materials, have been described with regard to their electrochemical properties for MSCs. We have summarized the recent progress in MSC based on well-developed 2D materials-based electrodes and its potential outcomes with different architectures including interdigitated pattern, stacked MSC and 3D geometries for on-chip electronics. This chapter provides a brief overview of the recent developments in the field of 2D material based all-solid-state microsupercapacitors (MSCs). A brief note on the MSC device configuration and microfabrication methods for the microelectrodes have been discussed. Taking advantage of certain 2D materials such as 2D MXenes, TMDs, TMOs/TMHs that provide good surface chemistry, tunable chemical and physical properties, intercalation, surface modification (functionalization), heterostructures, phase transformations, defect engineering etc. are beneficial for enhancement in pseudocapitance as it promotes the redox activity.

Keywords: microsupercapacitors, solid-state supercapacitors, two-dimensional materials, energy storage

1. Introduction

The popularization of portable electronic equipment has concentrated heavily on miniaturization and convergence of different technologies. While technologies such as wearable sensors and flexible displays has progressed, advances in energy storage are still lagging behind innovations in other electronic devices. Miniaturization of energy sources is also essential for environmental, medical, biological and other applications. Consequently, the reduction in size and integration of micro-power systems such as micro-batteries, micro-fuel cells, micro-supercapacitors (MSCs) and piezoelectric power harvesters are essential for the

future growth of portable electronic devices [1]. MSCs have gained considerable attention among these micro-power systems due to its high power densities, fast rate capabilities, ultra-long – cycle life and simple integration into the micro-nano electronic system as energy sources [2, 3]. Three main types of device configurations for MSCs have been developed to date: in-plane architecture, fiber shape and three-dimensional (3D) type (**Figure 1**). The advantages and disadvantages of these device configurations are given in **Table 1**. The performance of MSCs is determined not only by components but also by the combination of each individual element for the development of a device.

The choice of electrode materials and electrolytes is the two critical parameters influencing the electrochemical performance of the MSCs. Two-dimensional (2D) materials with unusual properties such as ultra-thin thickness, large lateral size, excellent flexibility and tunable physicochemical properties are currently the perfect choice for MCS as an electrode material. A large number of 2D materials have been developed to date, including graphene and analog nanosheets such as transition metal dichalcogenides (TMDs), transition metal oxides/hydroxides (TMOs/TMHs), metal carbides and nitrides (MXens), boron nitride (BN), phosphorene, and so on. In addition to electrode material selection, the electrolyte selection also plays a crucial role in the performance of MSC and these electrolytes can be classified into two types (i) conventional liquid electrolytes and (ii) solid-state electrolytes [9]. Conventional liquid electrolytes have a common disadvantage in terms of their liquid nature; therefore, a strict encapsulation process is required to avoid electrolyte leakage. However, when the device is damaged, electrolyte leakage remains unavoidable. Accordingly, to overcome this disadvantage, a solid-state electrolyte was developed by blending the acids, ionic liquids and salts into a polymer matrix. Several polymer matrixes have been used in solid-state electrolytes, including poly-(vinylidene-fluoride) (PVP), polyacrylonitrile (PAN)

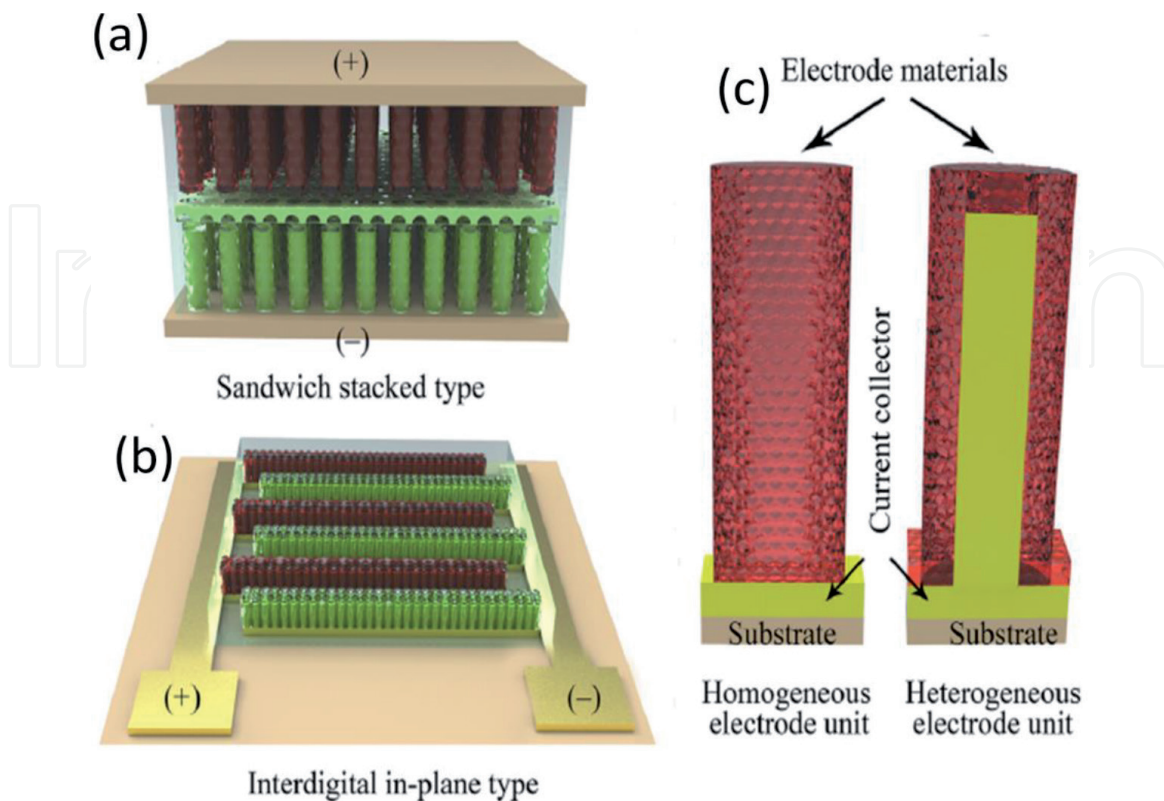


Figure 1. Schematics of three major MSC architecture (a) stacked architecture (b) Interdigital finger electrode architecture (c) cross-section of electrodes [4].

| Device configuration | Advantages | Disadvantages |
|------------------------|--|--|
| In-plane architecture | <ul style="list-style-type: none"> • They consist of interdigital electrodes with many dense micro-fingers, where the counter electrode interspaces are small enough for the transport of ions so that the devices have little impedance, high capacity and quick frequency responses [5]. • Ease of integration with other microelectronics. • This design can make the active electrodes more accessible because they are exposed to electrolytes on the edges. Therefore high power density can be achieved with batteries and supercapacitors. • This design contributes to the separator elimination [6]. | <ul style="list-style-type: none"> • The geometric parameters of the electrodes still have to be optimized. |
| Fiber-shaped | <ul style="list-style-type: none"> • Generally small in size and lightweight. • Thanks to their unique wire-shaped structure, they are highly flexible and can be woven or knitted with excellent wearability [7]. • Excellent versatility and can be produced in different shapes and different locations [8]. | <ul style="list-style-type: none"> • It cannot compete in terms of energy density with micro-batteries as energy storage equipment; large scale application is a big challenge [8] |
| Three-dimensional type | <ul style="list-style-type: none"> • This design maximize the energy density of MSCs • The volume of electrolyte utilized is further reduced with this design, leading to enhanced volumetric/areal energy density [4]. | <ul style="list-style-type: none"> • Require a series of complex micro-fabrication techniques. • Designing of 3D type MSCs with leakage-free electrolyte is still a challenge [4]. |

Table 1.
Advantages and disadvantages of various MSC device configurations.

and poly-(vinyl-alcohol) (PVA) [9]. These electrolytes can provide long cycle-life, low leakage current, high ionic conductivity and high mechanical flexibility. For example, the ionic conductivity of PVA/H₃PO₄ is about 10⁻³ Scm⁻¹, while the ionic conductivity PVA/H₂SO₄ can be even higher, about 7 x 10⁻³ Scm⁻¹. However, aqueous solid-state electrolytes suffer from a low voltage window at about 1 V due to the electrolysis voltage of water similar to aqueous electrolytes. A high operating voltage of 2.5 V can be achieved for micro-supercapacitors through ionic liquid solid-state electrolytes, resulting in a high energy density in sequence [10]. They also allow additional functionality, such as flexibility and stretchability, in addition to easy encapsulation. Considering these advantages, the choice of solid-state electrolytes in micro-supercapacitors is more reasonable.

2. Microfabrication technologies for microelectrodes of MCSs

This technology used for the fabrication of microelectrodes of MCSs can be grouped into two categories. The first categories include direct electrode material synthesis on the patterned current collectors using laser scribing, CVD, electrolytic deposition and pyrolysis. The second category consists of indirect manufacturing using existing electrode materials in powder or solution form.

| Methods | Advantage | Disadvantage |
|-----------------------------------|---|--|
| Chemical vapor deposition (CVD) | Controlled design and structure [2] | Expensive, time-consuming process, low mass loading and vigorous reaction condition (2). |
| Electrolytic deposition | Simple, efficient, cost-effective, environmentally friendly and large scale-production [2, 11] | Uncontrolled lateral direction growth [2]. |
| Electrophoretic deposition | Cost-effective, simple, thickness can be controlled [2, 11]. | Restricted by the species charged [2]. |
| Inkjet printing | Cost-effective, fast process, low mass loading, precise thickness control, direct patterning, large scale production, fair resolution (around 50 μm) enhance the resolution and scalability because no manual assembly is required during device manufacturing [2, 12]. | Ink preparation is a complicated process, limited by resolution, jam of nozzle [2, 10]. |
| Screen printing | Low-cost, scalable and fast process | Low resolution |
| Photolithography (UV lithography) | Cost-effective with high control precision [10], simple fabrication process [9], can produce uniform and accurate large-area samples [13]. | A sacrificial template is required; hence it's a complicated process, long preparation time [9]. |
| Drop, spin and spray coating | Facile, simple, thickness-control, large-scale fabrication, time and energy saving [2]. | Low-production efficiency and heterogeneous [2]. |
| Vacuum filtration | Low- cost, simple, convenient, thickness can be controlled [2]. | Shape and size is limited |
| Laser scribing | Cost-effective, scalable, simple, gives high throughput [9]. | Non-universal [2]. |
| Layer-by layer assembly | Multilayer films can be easily prepared, cost-effective and straightforward method, high resolution [14]. | Time-consuming process |
| Pyrolysis | Single-step synthesis [2]. | Complex and high-temperature process [2]. |

Table 2.
Microfabrication techniques for fabrication of MSCs.

The advantages and disadvantages of various techniques developed are explained below in **Table 2**.

No strategy in the fabrication of MSC microelectrodes is yet dominant over the others. Therefore, improving existing assembly strategies and exploring new manufacturing methods to overcome those limitations has become essential. In the meantime, to select appropriate assembly strategies to achieve high-performance MSCs, consideration should be given to overall factors such as active electrode materials, electrolytes, and interface between electrolytes and micro-electrodes [15].

3. Performance metrics of MCSs

The parameters used generally to assess supercapacitors' performance against volume and weight units are gravimetric capacitance, energy, and power. It is important to note that the supercapacitors gravimetric capacitance varies according to total

density, mass and thickness of the electrode, and other components' weight. So it's hard to compare the various MSC based on gravimetric capacitance [16]. But this parameter is not suitable for planar MSC where electrode material's weight is insignificant and the device's volume and surface area are always limited. Since the overall mass load of active materials in MSCs is small, the volumetric performance and, more significantly, the areal performance are more adapted for electrochemical performance [17].

Since equipment need to be integrated with miniaturized electronic devices with limited area, a performance assessment against the footprint area of MSCs is essential. Therefore areal capacitance, power density and energy density are the more reliable parameters for MSC performance monitoring. These parameters can be calculated using the equations given below [17].

$$C_s = \frac{Q}{s\Delta V} \quad (1)$$

$$E_s = \frac{0.5 C\Delta V^2}{3600 s} \quad (2)$$

$$P_s = \frac{\Delta V^2}{4s ESR} \quad (3)$$

Where C_s is the areal capacitance in F/cm^2 , 's' is the total area of microelectrode array and ΔV is the voltage range. P_s and E_s is the maximum power and energy density. The essential parameter to detect the electrode's areal performance is to measure the total area accurately.

4. Two- dimensional materials for MCSs

A promising material for the production of MCSs is Planar 2D molecules of atomic thickness with a large specific surface area. The reduced dimension of these materials also satisfies the miniaturization requirements of device size, offering new possibilities for high-performance MSC development [18, 19]. The material properties of this rich family consisting of graphene, transition metal oxides (TMOs), transition metal chalcogenides (TMDs), metal carbides and nitrides (MXene), black phosphorus (BP), etc., range from superconducting, metallic, semiconducting and insulating behavior due to its diverse electronic structure, offering a wide range of material solutions to achieve high-performance. The essential reasons why 2D material based solid-state MSC are essentials is enlisted below

- Excellent electrical conductivity

The essential qualification for high-performance MCS electrode materials is the excellent electrical conductivity, which can accelerate the adsorption and desorption of the charges and increase the diffusion rate of ions. This electron transport behavior is very closely linked to the electronic crystal structure, resulting in three typical insulating, semiconducting, and metallic transport behaviors. In general, metallic 2D materials, such as TMDs, have good electrical conductivity and several other 2D semiconductors like graphenes and BPs also offer favorable electron transport characteristics [19].

- Excellent-electrochemical activities

The electrochemical activity of some 2D material would be useful for the redox reaction to further increase the pseudocapacitance. The promising electrode material of microsized pseudocapacitors, which generally display high capacitance performance, is proven to be 2D MXenes, layered double hydroxides (LDHs), metal oxides and hydroxides with excellent electrochemical properties [19].

- Large surface area

The extra-large surface area offers an energy storage platform with huge active sites to increase the electrochemical activity and charge adsorption, thus making 2D metal-organic frameworks (MOFs) and covalent organic frameworks (COFs) with inherent porosity a promising MSC functional electrode material [19].

- Mechanical flexibility

Superior mechanical flexibility at the atomic level and a diverse array of various 2D nanosheets provide desirable flexibility and multiple functionalities [15].

4.1 Graphene

Graphene is the most widely studied electrode material for MSCs due to its excellent electrical conductivity, large specific area, chemical stability, excellent intrinsic double-layer capacitance of approximately $21 \mu\text{F}/\text{cm}^2$ and theoretical capacitance of around 550 F/g [20–22]. Several reviews of graphene-based MSCs have been published. Zhang *et al.*, Xiong *et al.* tried to summarize the recent developments in graphene-based MSCs and the methods employed to produce high-performance MSCs [20, 21]. Similarly, Wu *et al.* classified graphene-based MSCs and provided a complete overview of on-chip graphene-based planar interdigital MSCs [21]. Gao *et al.* recently provided an overview of the MSC system's application, based on 1D, 2D and 3D graphene [23].

Several strategies were employed to enhance the electrochemical performance of graphene-based MSCs. The first approach was to improve the charge storage capacity of electrode materials by preparing graphene composites with other pseudocapacitive materials [11, 24, 25] or doping graphene with heteroatoms like boron [26] and fluorine [27]. The second approach consists of constructing an asymmetric structure [11, 25] and the third approach was to increase the loading quantity of active electrode materials by 3D electrode construction on the confined area of MSC [17]. To realize this 3D electrode construction, Wang *et al.* used a 3D printing technique to fabricate an all-solid-state flexible MSC using nitrogen (N)/oxygen (O)-doped graphene ink. This device shows a high power density of 0.23 mW cm^{-2} and an areal energy density of $2.59 \mu\text{Wh cm}^{-2}$, excellent cycling stability, and good mechanical flexibility. This increase in electrochemical properties observed due to three reasons (i) increased surface area due to the doping with N and O (ii) enhanced hydrophilic property of N/O doped graphene ink (iii) increased electrical conductivity as well as the pseudocapacitive effect of O and N doping [28]. Like this study, Szymon and his group developed a new type of polyaniline (PANI) anchored pseudocapacitive MnO_x passivated graphene microflake inks and manufactured a solid-state MSC using the inkjet printing technique in a 3D configuration given in **Figure 2**. This ink shows excellent stability and jetting performance that may be due to the dual-passivation process employed here. For the first time, this is to report such a fully inkjet-printed MSC with 3D electrode configurations

with excellent rate performance and stability. However, these microflake inks have been developed based on the self-assembly behavior of 2D materials following Rehani *et al.*'s [30] 3D coarse-grained lattice gas model [29]. Toan *et al.* built an on-chip MSC where the electrode consists of silicon nanowire-graphene nanowall-PANI ternary composite. Here the silicon nanowire template with a high aspect ratio is fabricated using the metal-assisted chemical etching (MACE) technique. On this silicon nanowire, 3D hierarchical graphene nanowalls were produced using microwave plasma-enhanced chemical vapor deposition (PECVD), which significantly improves the electrochemical performance of the manufactured MSC. However, this solid-state 3D MSC delivers an areal energy density of about $10.8 \mu\text{Wh}/\text{cm}^2$ and a power density of about $0.78 \text{ mW}/\text{cm}^2$ [31]. Lu *et al.* chose asymmetrical arrangement and produced an in-plane asymmetric interdigitated MSC using mask-assisted vacuum filtration techniques, among the various strategies discussed to improve graphene performance. They develop this asymmetric MSC based on an all-graphene system, where both the working electrodes are graphene derivatives. Using the same chemical composition and microstructure electrodes enhances performance and helps avoid power imbalance that conventional hybrid and asymmetric systems usually encounter [32]. Therefore, the anode of this MSC is made of functional graphene oxide (FGO), while the cathode consists of functional reduced graphene oxide (FrGO). This FGO, which is electrochemically exfoliated from graphite papers, has enhanced hydrophilic properties compared to pristine graphene, difficult to disperse in water [33]. FGO has abundant functional groups responsible for the hydrophilic properties of the FGO, leading to the formation of wrinkles on its surfaces. However, this asymmetric MSC has the highest surface capacitance of approximately 7.3 mF cm^{-2} in PVA/ Na_2SO_4 electrolyte. The high performance of this MSC is attributable to abundant functional group doping

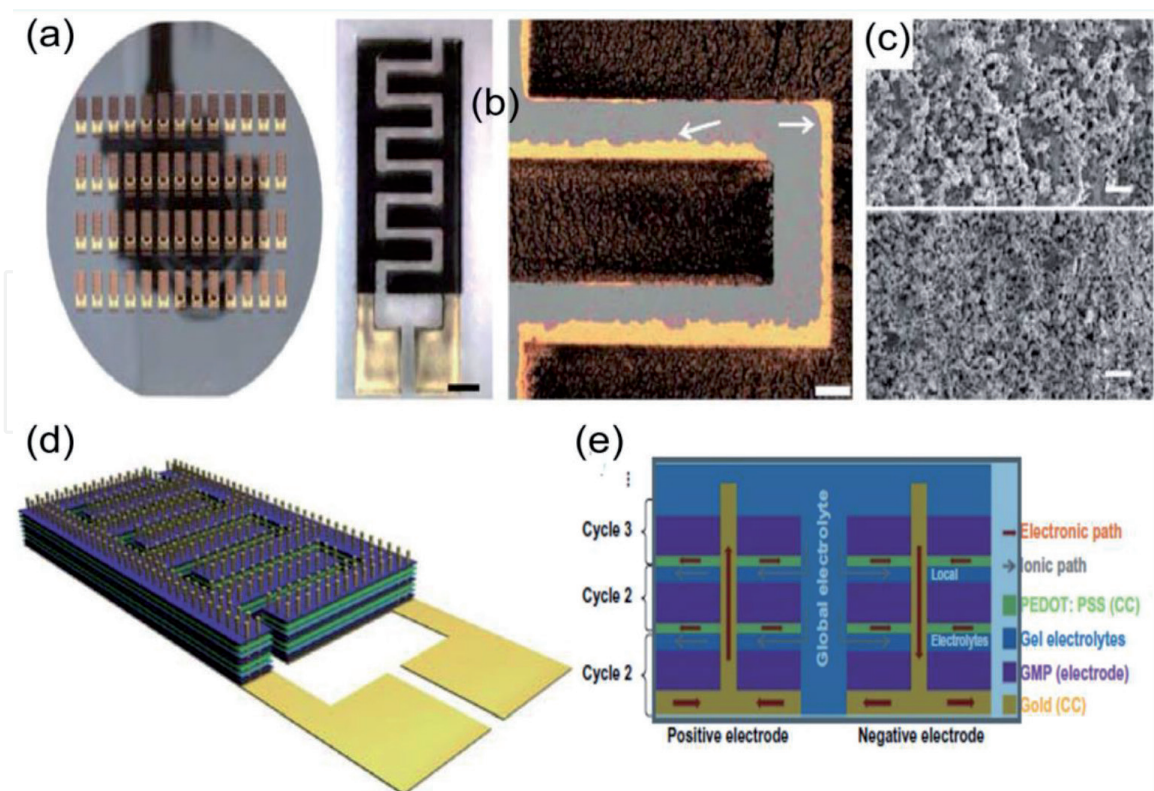


Figure 2. Inkjet-printed GMP (doped graphene passivated flakes) MSC developed by Delekta *et al.* (a) Photograph of inkjet-printed MSC (b) micrographs of printed GMP MSC on glass substrate (c) SEM images of patterned GMP MSC (d and e) 3D heterogeneous GMP MSC [29].

and heteroatom substitution with graphene elements N, O, P, S, and the in-plane interdigitated architecture. This MSC has demonstrated exceptional flexibility, showing the feasibility of the wearable application of the MSCs [34].

Lochmann *et al.* reported a stamping approach combined with soft lithography for MSC production for the first time, but this approach is time-consuming and not appropriate for producing PET and paper-based MSC [35]. Zhang *et al.* subsequently made a flexible MSC based on MXene in a paper substrate using a stamping method, but even this MSC suffered from lower areal and volumetric capacitances [36]. To this end, Esfahani and Khosravi reported the manufacture of a graphene-based flexible MSC using a single-step stamping method on a PET-coated parafilm using a pre-designed pattern. This imprinted parafilm-coated PET pattern was filled with graphene oxide (GO)/MnO₂/carbon aerogel hybrid paste, which acts as a binder and additive-free active material and finally, with the help of nascent hydrogen GO reduction is made. This type of GO reduction improves stability and reduces the ohmic resistance of the prepared electrode. The active material, i.e., G/CA/MnO₂ used here, exhibits a unique morphology that enhances the electrochemical surface area and facilitates the diffusion of electrolytes ion. The edged structure of graphene also helps to improve the electrochemical activity and capacitance of the SC. Based on the Hota *et al.* [37] inferences, they also used fractal design of large and small finger widths and compared their performance with ID electrodes. The small finger width fractal design (SFWF) shows high areal and volumetric capacitance of around 14.2 mF cm⁻² and 71.3 Fcm⁻³ among these different electrode designs. This method proves feasible in designing various low-cost architectures and improves the flexible-graphene performance based on MSC, which has been reported to date. The manufacturing process of this flexible MSC provides a new direction in the modification of the substrate and the current collector and the manufacturing method and the method of graphene reduction. This MSC fabricated by this stamping method also demonstrates excellent flexibility, reflecting its potential in future flexible electronic devices [38]. The presence and regulation of the functional group are essential for improving the performance of the graphene-based MSCs. These functional groups not only provide active pseudocapacitance sites, but they also prevent the aggregation of graphene without affecting both wettability and conductivity of graphene. To date, several strategies have been reported for regulating graphene functional groups, such as the treatment of O₂ plasma, laser power, etc. However, it is worth working on regulating the functional groups of graphene to balance the active site, electrical conductivity, and wettability, which have plenty of room for further performance improvement in MSCs. Consequently, to improve the electrochemical efficiency of reduced graphene oxide (RGO), an appropriate method of controlling the functional group is required. Based on these facts, Wu *et al.* fabricated a free planar MSC using symmetric graphene-based metal current collector, where the functional groups were regulated using both air-plasma treatment and exposure to blue violet-laser (BV-laser) as shown in **Figure 3a**. The XRD pattern of the prepared composite is shown in **Figure 3c** and it can understand from the figure that this BV-laser treatment and air-plasma treatment do not change the phase structure of RGO. The interlayer spacing calculated for this composite is higher than that of graphite structure, which indicates a π - π stacking between graphene sheets in these composites. These combined techniques balance the pseudocapacitance active sites, conductivity and wettability by tuning the functional groups on the graphene surface and the possible transformation pathway is shown in **Figure 3b**. The CV curves of this material are shown in **Figure 3d** exhibit a symmetric-quasi rectangular state that demonstrates that this material's capacitive behavior is due to the simultaneous pseudocapacitive and electrical double layer behavior (EDL). This symmetrical solid-state MSC exhibit excellent energy density

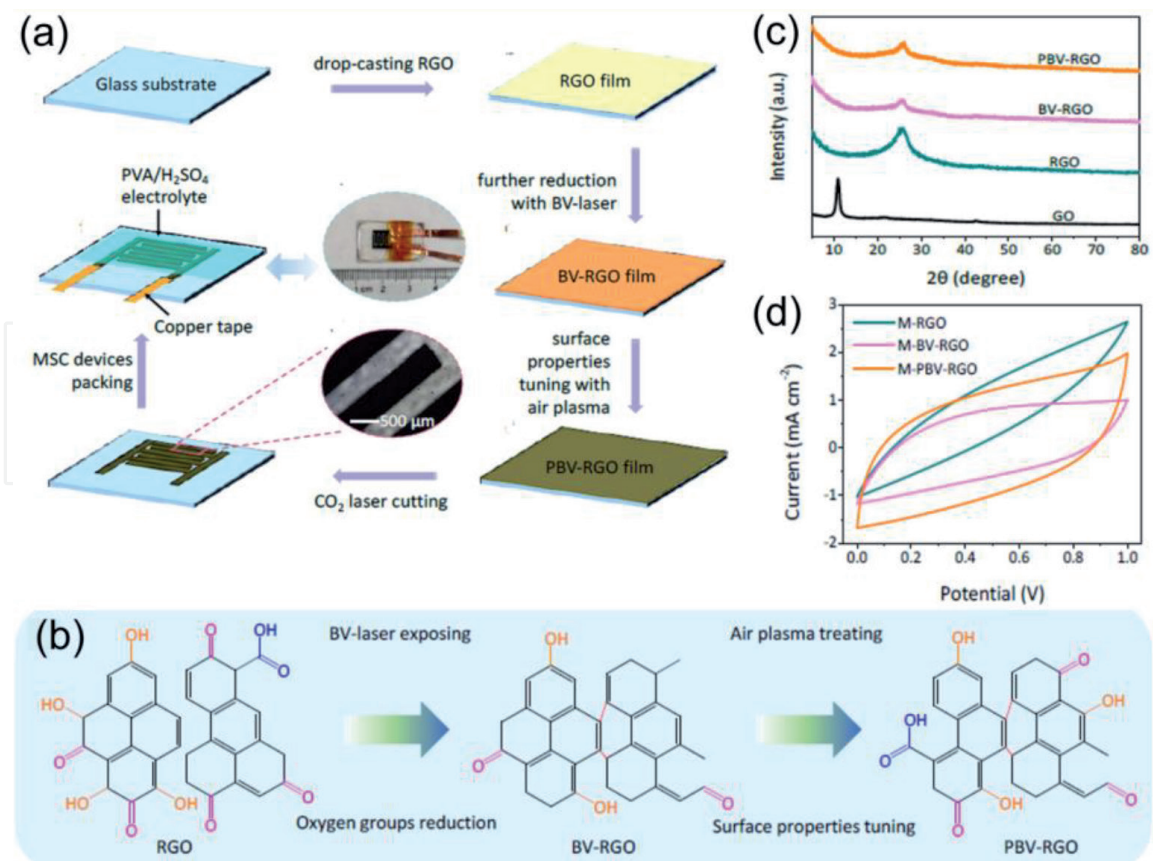


Figure 3. (a) Fabrication steps involved in the manufacturing of in-planar PBV-RGO MSC developed by Wu *et al.* (b) the suggested pathway transformation of RGO on exposure with BV-laser exposing and air-plasma treatment to produce PBV-RGO electrode material (c) XRD pattern of PBV-RGO electrode material (d) CV curves of RGO (M RGO) after BV-laser treatment (M BV-RGO) followed by air-plasma treatment (M-PBV-RGO) [39].

and power density around $2.49 \mu\text{Wh cm}^{-2}$ and 5 mW cm^{-2} and superior long term stability after 10,000 cycles with 99% retention, which exceeds most reported all-solid-state graphene-based MSCs. This manufacturing method is suitable for the process of micro-integrated circuit machining and has an enormous potential in the production of on-chip devices [39]. Liu *et al.* adopted a new series of inter-digital setups without any internal connection by combining techniques such as photolithography and liquid-air interface self-assembly methods. This solid-state planar on-chip MSC without internal connection shows excellent cyclic stability and outstanding energy and power density. This work demonstrates that graphene-based planar on-chip MSCs with no internal connection can integrate better with electronic components [40].

4.2 Transition metal dichalcogenids (TMDs)

Single or few layers TMDs have attracted considerable attention because of their tunable band gaps and extensive natural reserves [2]. These compounds show a typical MX_2 formula, where M is an element in Group IV-VI metal, and X is a chalcogen (S, Se, or Te). In this case, Stoichiometry relies on the process and the strategy of producing a compound made up of transition metal and chalcogen elements. The layered TMDs are typically 6 to 7 Å thick and consist of an X-M-X hexagonal sandwich with a metal-atomic layer separated by both layers of chalcogen [41]. The physical properties of bulk TMD's vary from true metals such as VSe_2 and TaS_2 , semi-metals such as WTe_2 and TiS_2 , semiconductors such as MoS_2 and

SnS₂ and insulators such as HfS₂. Suitable electrode materials for MSCs are among these metallic TMDs with large surface area and high conductivity [2].

MoS₂ can effectively store charges over a single atomic layer utilizing an inter and intrasheet double layers. Here the central atom Mo shows an oxidation state ranging from +2 to +6 and shows a pseudocapacitive behavior with a theoretical capacitance of about 1000 F/g. But aggregation and low electrical conductivity between the atomic layers of MoS₂ hinder their extensive use in MSCs. Hybridization of TMDs with carbon material, which provides quick-electron transport and more active-sites, is one approach to solve these problems. Hence Yang *et al.* reported a solid-state MSC using MoS₂@rGO– photoresist-derived carbon-nanotube (CNT) hybrid composite by spin coating followed by photoetching and pyrolysis similar to the MoS₂@sulfonated rGO hybrid prepared by Xiao *et al.* shown in **Figure 4** [42]. This hybrid prepared by Yang *et al.* was then embedded in carbon microelectrodes, which synergistically increase the performance of the MSCs and exhibited high energy density (5.6 mWh cm⁻³) as well as areal capacitance (13.7 mF cm⁻²) with good capacitance retention [43]. Similarly, Haider *et al.* have reported other carbon microelectrodes based on TMD using the advantages of metallic VS₂. The high energy density (15.6 mWh cm⁻³) and specific capacitance (86.4 Fcm⁻³) result from the synergistic combination of VS₂ and carbon. This system exhibited excellent energy density and power density compared with the energy storage system developed by Xiao *et al.* and Yang *et al.* [44]. Besides constructing MoS₂ hybrids with conductive carbonaceous material, the phase modification in which the Mo coordination changes from the trigonal prismatic (2H) phase to the octahedral (1T) phase is another practical approach to improve the electrochemical performance of MoS₂ [45]. Very recently, Xu *et al.* reported a femtosecond laser direct writing technique to fabricate an MSC based on 1T MoS₂. This is the first time an MSC with excellent performance based on 1T MoS₂ has been reported. These femtosecond lasers can help achieve a submicron resolution (~800 nm), which is nearly 40 times more accurate than that achieved with traditional nanosecond lasers with a resolution of around 10-200 μM. This approach is green, facile, maskless, flexible and high vacuum environments are not required. The electrochemical performance and

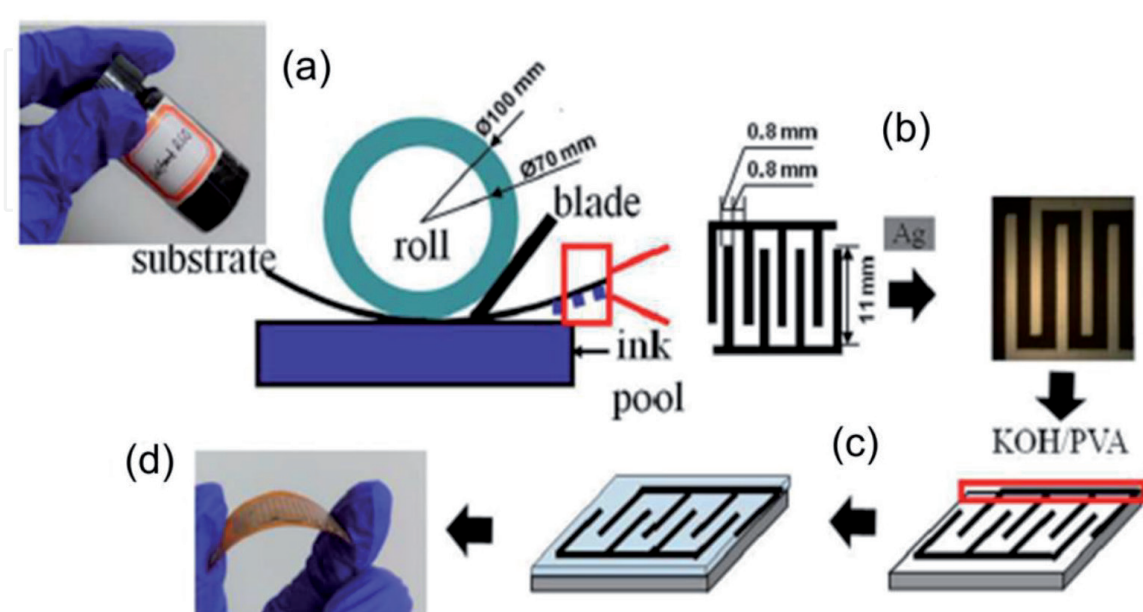


Figure 4. (a) Schematic picture of fabrication of MoS₂@SrGO MSC using gravure printing techniques (b) photograph of prepared MSC after Ag paste painting (c) KOH-PVA gel electrolyte coated on gravure printed electrode (d) MoS₂@SrGO printed electrode in PI substrate. (Source: Reprinted from [42]).

the MSC resolution are enhanced by lowering the thermal effect to regulate the phase transition of these 1 T MoS₂ based electrode material. This MSC with in-plane configuration results in high-frequency response with ultrafast ion-diffusion rate, high specific capacitance, good cycle-life, low equivalent series resistance (ESR) value, unprecedented power density (nearly 14 kW cm⁻³) and high energy density (15.6 mWh cm⁻³) in PVA/H₂ SO₄ electrolyte. However, this MSC with a surface area of 100 × 100 μm² and a high-frequency response and time constant are suitable for AC line filters and other electronic devices demanding high power requirements [46].

The fabrication of supercapacitors with excellent energy storage capacity and flexibility in wearable smart electronics has recently attracted significant attention. Thus, a fabric supercapacitor using low-cost textile fabrics with good mechanical properties and biocompatibility coated with ternary composite poly(3,4-ethylenedioxythiophene): poly(styrenesulfonate)/MoS₂/poly(3,4-ethylenedioxythiophene) (PEDOT: PSS/MoS₂/PEDOT) is manufactured by Chen and the group. This all-solid-state fabric MSC was fabricated by vapor phase polymerization (VPP) and the vapor phase deposition method exhibits an energy density of around 1.81 mWh/cm³ and power density of around 0.82 W/cm³. The fabric coated with this ternary composite has a 3D configuration with interconnected structure and exhibits a large surface area that enables fast electrolyte transport and provides active electrolyte accessibility. This MSC assembled in a belt-shaped device was also used by the group as transient power sources to operate the light-emitting diodes [47]. Very recently, Li *et al.* printed a MoS₂ based all-solid-state in-plane MSC using inkjet printing. This MSC printed with MoS₂ based inks has high loadings of active materials per unit area resulting in a thinner and more flexible supercapacitors than the conventional sandwich structure. PEDOT: PSS inks were first printed on PI substrate to improve the conductivity, followed by printing of MoS₂ based inks subsequently to fabricate the MSC. This scalable synthesis technique is demonstrated in **Figure 5a**. The SEM image (**Figure 5b**) shows that the layered MoS₂ formed a uniform 2D conductive network above the pre-printed PEDOT: PSS electrode, which differs from the morphology observed in the ternary composite prepared by Chen and group. They also demonstrated the relationship with the increase of electrode thickness vs. conductivity in **Figure 5c** and its practical application by powering an LED bulb by connecting MSC in series combination [48].

4.3 MXenes (Ti₃C₂T_x)

The overall performance of MSCs is based on the intrinsic properties of electrode materials. In many cases, carbonaceous materials such as graphene [49, 50], graphene oxide [51], CNTs [52, 53], carbide-derived carbon [54, 55] and their hybrids [56, 57] with charge storage via electric double layer, were reported in MSCs. Later, high capacity MSCs based on pseudocapacitive materials such as conductive polymers [58], transition metal oxides/hydroxides [59, 60] and sulfides (VS₂, MoS₂) [61, 62] with surface redox reactions were reported. Nevertheless, the poor electrical conductivity and lower packing density of electrode materials in these MSCs restrict the accessible volumetric and areal capacitances, the two important parameters used to indicate the performance of MSCs [63]. Recently, MoS₂ with high packing density served as a good electrode material to fabricate energy storage devices characterized by high power densities and volumetric energy [64]. A new group of layered 2D materials called MXenes, which includes transition metal nitrides, carbides, and carbonitrides, was recently reported.

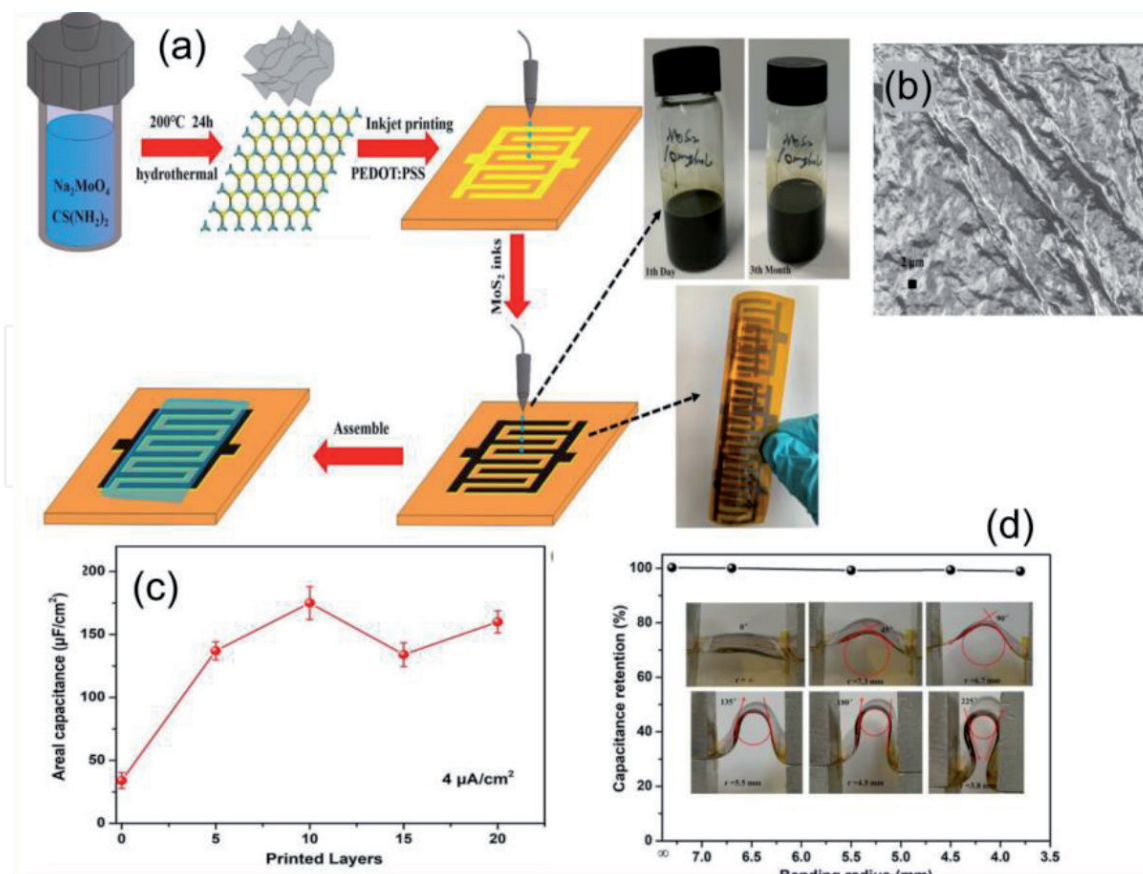


Figure 5.

(a) Steps involved in the fabrication of flexible MSC using MoS₂ inks by inkjet printing (b) SEM image of printed MSC in PI substrate (c) relationship between areal capacitance vs. number of printed layers (d) capacitance retention under different bending radius of the fabricated supercapacitor [48].

MXenes are promising layered materials derived from the precursors with the general formulae $M_{n+1}AX_n$ (M refers to Ti, Sc, Nb etc.; A = Al, Sn, Si, etc.; $n = 1, 2, 3$). In the MAX phase, the M layers are hexagonally close-packed and MXenes can be synthesized by selective etching of A element from the MAX phase using acidic-fluoride-containing aqueous solutions [65]. The presence of an aqueous medium during the synthesis can create MXene flakes with various surface functional groups such as O, F, or OH. MXenes have characteristic properties such as rich surface chemistry, hydrophilicity, layered structure, high packing densities and intrinsic electronic conductivity. The first member $Ti_3C_2T_x$ was reported in 2011, opened up an exciting research field, as revealed by the increasing number of publications on MXenes [66]. The distinctive properties and simplicity of processing have contributed to various applications such as energy storage for supercapacitors and the maximum theoretical capacity was reported to be at $615Cg^{-1}$ [65]. The higher pseudocapacitance and simplicity of solution processing of MXenes are highly advantageous for the designing of MSCs that are used to power wearable electronics, sensors, and micromechanical systems with low power consumption. Various methods have been adopted to fabricate MXene based MSC patterns on the submillimeter scale. These are known to be potential candidate for the design of MSCs due to the following factors: 1) MXenes have an electrical conductivity up to $6500 S cm^{-1}$ [67], which permit fast electron transfer and excludes the requirement for current collectors like noble metals. 2) MXenes exhibit higher gravimetric capacitances relatable to graphene, with higher packing density up to $4 g cm^{-3}$ [68, 69], which needs to enhance the volumetric

characteristics (specific volumetric capacitance of 1000 F cm^{-3} for conventional three-electrode configuration [70], which is more than that of supercapacitors based on carbonaceous materials) [71].

Flexible MSCs are highly demanding to manufacture portable and on-chip energy storage devices because of their high security, lightweight and miniaturization [72]. Direct printing of functional inks is crucial for various applications such as smart electronic devices, healthcare, and energy storage. Nevertheless, currently available inks are distant from ideality. A low concentration of ink or the additives/surfactants are contained, which put on complexity to the fabrication and affects the printing resolution. Based on these facts, Zhang *et al.* demonstrated a direct printing method using two types of 2D MXene inks (aqueous for extrusion printing and organic for inkjet printing) to fabricate all-MXene MSCs with high resolution. The fabricated flexible MSCs displayed outstanding volumetric capacitance of 562 F cm^{-3} and a high energy density of $0.32 \mu\text{W h cm}^{-2}$, over all other printed MSCs reported yet. The approach of direct ink printing technique plays a major role beyond energy harvesting and storage applications, including sensors, circuits, and electronics, where simple, easily integrable and cost-effective components are required. This additive-free and low-temperature ink printing technique provides many applications in sensors, antennas, smart electronics and shielding [72]. Recently, Peng *et al.* adopted a solution spray coating and laser cutting to fabricate solid-state MSC based on interdigital L-s- $\text{Ti}_3\text{C}_2\text{T}_x$ film on a glass substrate in which two layers of MXene ($\text{Ti}_3\text{C}_2\text{T}_x$) with different flake sizes were obtained. The larger MXene flakes (L- $\text{Ti}_3\text{C}_2\text{T}_x$, 3–6 μm) were stacked to form a bottom layer which act as current collectors. The top layer contains smaller MXene flakes (s- $\text{Ti}_3\text{C}_2\text{T}_x$, 1 μm) with numerous edges and defects to form an electroactive layer for energy storage. The excellent electrochemical characteristics and homogeneity in structures could offer better cyclic performance and showed excellent areal capacitance of $\sim 27 \text{ mF cm}^{-2}$ and volumetric capacitance of $\sim 357 \text{ F cm}^{-3}$ at 20 mV s^{-1} . The L-s- $\text{Ti}_3\text{C}_2\text{T}_x$ MSC showed excellent cyclic stability after 10,000 cycles without any decay of capacitance at 50 mV s^{-1} . L-s- $\text{Ti}_3\text{C}_2\text{T}_x$ film on a glass substrate was transferred onto the scotch tape substrate shows good flexibility without prominent cracks after bending up to 100 times at an angle of 60° , the areal capacitances were comparable to its original rigid structure on a glass substrate. This approach opens up different designs for the fabrication of on-chip devices using different morphologies of MXenes and their composites, flake sizes, and chemistries [73]. The integration of flexible MSCs for on-chip energy storage applications still faces some challenges due to short cycling stability, complicated manufacturing processes, and low areal energy storage. To address this, Huang *et al.* utilized spray coating of MXene ($\text{Ti}_3\text{C}_2\text{T}_x$) conductive inks for the massive preparation of paper-based flexible MSCs by using a gel-like solid-state electrode (polyvinyl alcohol and H_2SO_4) and encapsulated layer of polydimethylsiloxane. As discussed above, a highly conductive and sprayable $\text{Ti}_3\text{C}_2\text{T}_x$ interdigitated electrode served the dual role of the current collector and active materials. This flexible MSC delivers a large areal capacitance of 23.4 mF cm^{-2} and an excellent cycling capability with a capacitance retention up to 92.4% over 5000 cycles, together with exceptional flexibility [74]. The crucial obstacles in MSC applications are short discharge time, low voltage output, and low current. MSC array is known to be a solution to avoid the obstacles mentioned above. Based on the capacitors' theory, the parallel connection will increase the capacitance while the series connection will decrease the output voltage corresponding to the capacitance decrease. It means a MSC array (combination of some MSCs) can increase both capacitance and output voltage [75]. Recently, a lightweight and freestanding MXene/bacteria cellulose composite paper with

outstanding electrochemical performance and mechanical stability through a facile all-solution based paper making method was fabricated by Jiao *et al.* Further, they adopted a laser-cutting kirigami patterning process for the fabrication of bendable, stretchable and twistable all-solid-state MSC arrays (Figure 6a). The structural design and excellent performance of MSC arrays could offer outstanding areal capacitance of 111.5 mF cm^{-2} and areal density of $0.0052 \text{ mWh cm}^{-2}$ with electrochemical stability under mechanical deformation. The photograph of a paper crane made from MXene/BC composite paper is shown in Figure 6b, it is used as a conductor for lighting LED (Figure 6c). This technique presented a promising method for designing and manufacturing excellent mechanically deformable MSC arrays based on MXenes [76]. For practical applications, the electrodes with a 3D structure can be easily destroyed via mechanical deformation. It is possible to improve MSC's energy storage ability by fabricating them in a 3D structure [77]. In this context, Yue *et al.* developed a self-healable 3D MSC comprised of r-GO and MXene ($\text{Ti}_3\text{C}_2\text{T}_x$) composite aerogel electrode with an outer shell of self-healable

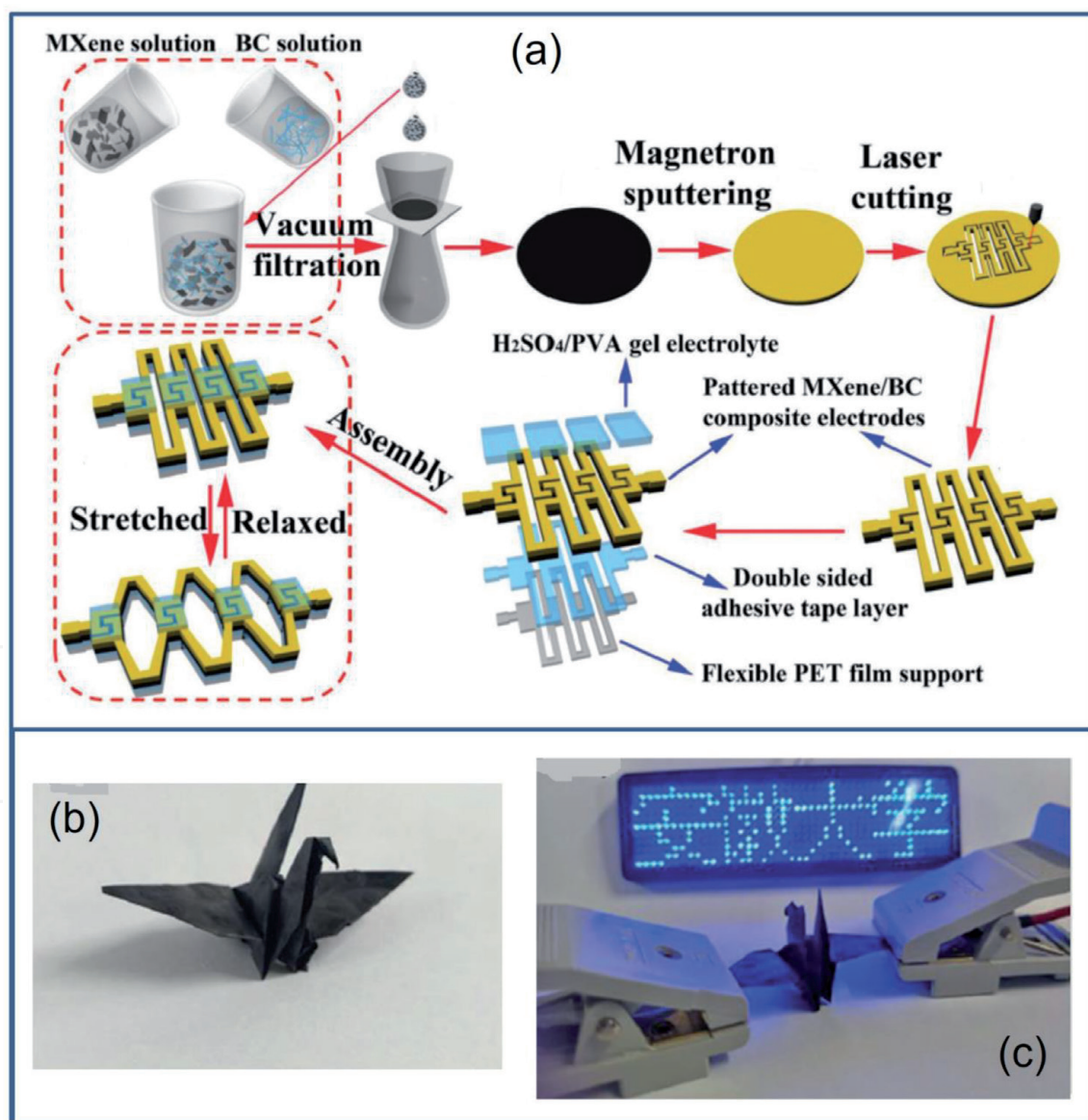


Figure 6.

(a) Schematic illustration of the manufacturing process of Mxene/bacterial composite papers and a laser-cutting kirigami patterning process for the fabrication of bendable, stretchable and twistable all-solid-state MSC arrays, (b) photograph of paper crane made from as-synthesized Mxene/BC, and (c) photograph of LED using paper crane working as conductor for lighting. (Source: Reprinted from [76]).

polyurethane through the ice-template method (**Figure 7a**). The composite aerogel electrode could resist the oxidation of MXene and prohibit the lamellar structure's restacking by combining the properties of components such as high conductivity of MXene and high surface area of r-GO. The fabricated MSC exhibited better performance with a large area-specific capacitance of 34.5 mF cm^{-2} at 1 mV s^{-1} , as shown in **Figure 7c-e**. The 3D-MXene-r-GO composite aerogel electrode displayed excellent cycling performance with 91% retention of capacitance after 15,000 cycles (**Figure 7f**). The 3D MSC maintained outstanding self-healing capacity (**Figure 7b**) with capacitance retention up to 81.7% after the 5th healing. The synthesis of self-healable 3D-MXene-r-GO MSC dispensed an approach for fabricating next-generation durable electronic devices with multi-functionality to meet sustainable development [77]. The performance of recently reported all-solid-state MSCs based on 2D materials are summarized in **Table 3**.

4.4 Other important 2D materials

Transition metal oxides/hydroxides (TMOs/TMHs) are electrochemical pseudocapacitor materials and widely used as electrode materials in supercapacitor applications due to their high energy density, abundance and high capacitance [87]. But their performance as supercapacitor electrode materials limited because of low intrinsic conductivity. So, 2D TMOs/TMHs have been explored in supercapacitors owing to their enhanced electronic conductivity and high specific surface area [88].

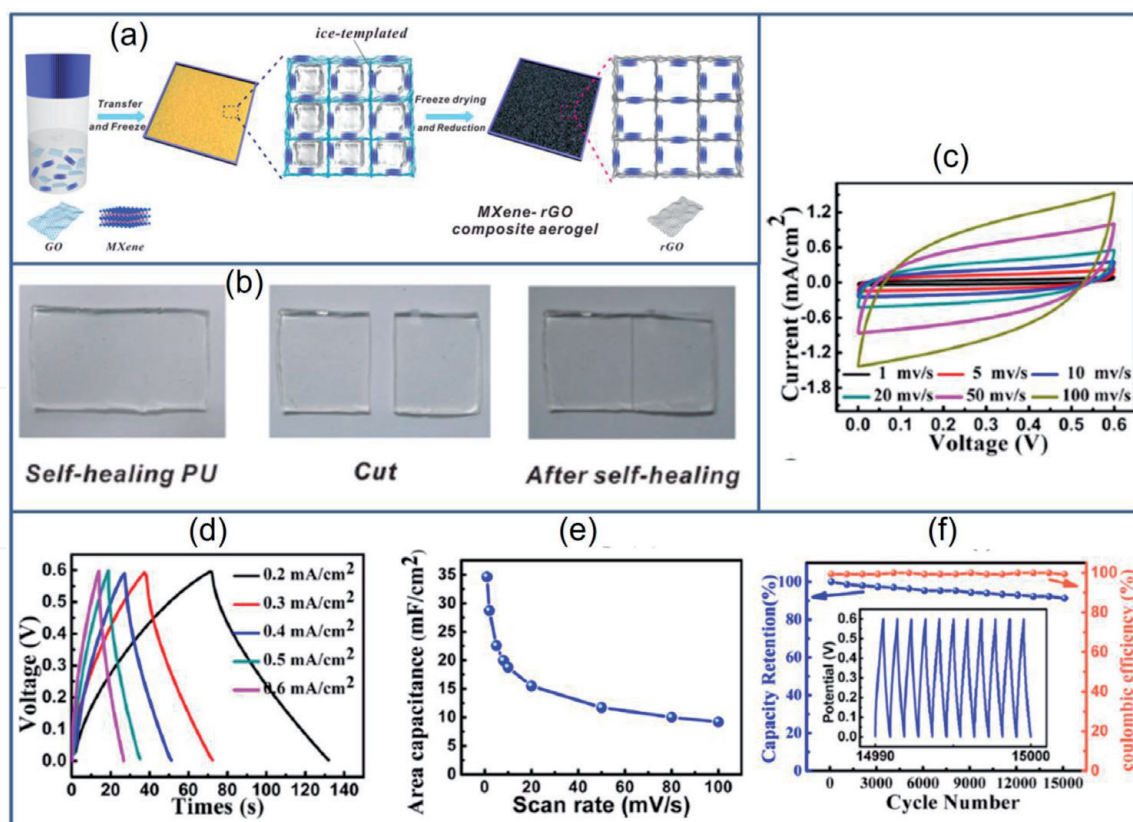


Figure 7. (a) Schematic illustration for the fabrication process of 3D MSC based on MXene-rGO composite aerogel, (b) photographs of the self-healable carboxylated polyurethane: Left (initial), right (after the healing) and middle (after damage). Electrochemical performance of MSCs based on the MXene-rGO composite aerogel (c) CV at various scan rates, (d) GCD at different current densities, (e) the variation in areal capacitances vs scan rate of MSC and (f) cycling stability of MSC based on MXene-rGO composite at the current density of 2 mA cm^{-2} . (Source: Reprinted from [77], with permission from, copyright@2018 ACS).

| MSC | Electrolyte | Voltage window (V) | Device performance | | Specific capacitance | | Cycling stability | Ref |
|--|--|--------------------|----------------------------|----------------------------|---------------------------|--------------------------------|---------------------------|------|
| | | | Power density | Energy density | Areal/mF cm ⁻² | Volumetric/ F cm ⁻³ | | |
| NOG-X-Y | PVA-H ₃ PO ₄ | 0 to 1 | 0.23 mW cm ⁻² | 2.59 μWh cm ⁻² | 18.70 | — | 93% after 10,000 cycles | [28] |
| GMP microflakes based 3D MSC | PVA/H ₂ SO ₄ gel | 0 to 1 | 10 mW cm ⁻² | 1 μWh cm ⁻² | 11 | — | 80% after 2000 cycles | [29] |
| Silicon nanowire-Graphene- PANI | PVA/H ₂ SO ₄ gel | -0.2 to 1 | 0.78 mW cm ⁻² | 10.8 μWh cm ⁻² | 77.7 | — | 75% after 2000 cycles | [31] |
| G/CA/MnO ₂ based ID patterned MSC | PVA/H ₂ SO ₄ gel | 0 to 1 | 43.2 μW cm ⁻² | 1.2 μWh cm ⁻² | 8.7 | — | 85% after 5000 cycles | [38] |
| M-PBV-RGO | PVA/H ₂ SO ₄ gel | 0 to 1 | 5 mW cm ⁻² | 2.49 μWh cm ⁻² | 21.86 | — | 99% after 10,000 cycles | [39] |
| Graphene based integrated planar on-chip MCS | PVA/H ₂ SO ₄ gel | 0 to 2 | 68.268 mW cm ⁻³ | 3.792 mWh cm ⁻³ | — | 2730 | 89% after 10,000 cycles | [40] |
| MoS ₂ @S/rGO | KOH-PVA gel | | 13.4 mWcm ⁻³ | 0.58 mWh cm ⁻³ | 6.56 | — | 91% after 1000 cycles | [42] |
| MoS ₂ @rGO/CNT | PVA/H ₂ SO ₄ gel | 0-1 | — | 5.6 mWh cm ⁻³ | 13.7 | — | 96.6% after 10,000 cycles | [43] |
| C/VS ₂ | | 0-1.2 | 2.88 Wcm ⁻³ | 15.6 mWh cm ⁻³ | — | 86.4 | 97.7% after 10,000 cycles | [44] |
| 1 T MoS ₂ (t-If laser) | PVA/H ₂ SO ₄ gel | 0-0.5 | 14 kW cm ⁻³ | 15.6 mWh cm ⁻³ | 36 | — | 93% after 5000 cycles | [46] |
| PEDOT: PSS / MoS ₂ / PEDOT | PVA/H ₃ PO ₄ gel | -0.2 to 1 | 0.82 W/cm ³ | 1.81 mWh/cm ³ | 1.43 | — | 93.6% after 5000 cycles | [47] |
| Inkjet printed MSC based on MoS ₂ | PVA/H ₂ SO ₄ gel | 0 to 0.6 | 0.079 W cm ⁻³ | 0.215 mWh cm ⁻³ | — | 175 μF/cm ³ | 85.6% after 10,000 cycles | [48] |

| MSC | Electrolyte | Voltage window (V) | Device performance | | Specific capacitance | | Cycling stability | Ref |
|---|--|----------------------|---|--|---------------------------|--------------------------------|--|------|
| | | | Power density | Energy density | Areal/mF cm ⁻² | Volumetric/ F cm ⁻³ | | |
| 2D Ti ₃ C ₂ T _x /PDMS | PVA-H ₂ SO ₄ | 0 to 0.6 | 189.9 mW cm ⁻³ | 1.48 mW h cm ⁻³ | 23.4 | — | 92.4% After 5000 cycles | [68] |
| PANI/EG/ Ti ₃ C ₂ T _x | PVA-H ₃ PO ₄ | 0 to 0.7 | 159.6 mW cm ⁻³ 2015 mW cm ⁻³ | 2.3 mWh cm ⁻³ 1.3 mWh cm ⁻³ | — | 36.4 | 90% After 8000 cycles | [78] |
| Ti ₃ C ₂ T _x -PET | PVA-H ₃ PO ₄ | 0 to 0.6 | 225 mW cm ⁻³ 744 mW cm ⁻³ | 2.8 mWhh cm ⁻³ 2.3 mWh cm ⁻³ | 23 25.5 | — | 76% after 10,000 cycles | [79] |
| Ti ₃ C ₂ T _x /polymer electrolyte (PE) | PVA-H ₃ PO ₄ | 0 to 0.8 | 8 mW cm ⁻² | 28 μWh cm ⁻² | 276 | — | 95% After 1000 cycles | [80] |
| Extrusion printed MXene Inkjet printed MXene | PVA-H ₂ SO ₄ PVA-H ₂ SO ₄ | 0 to 0.5 0 to 0.5 | 11.4 μW cm ⁻² - | 0.32μWh cm ⁻² - | 43 12 | - 562 | 97% After 10,000 cycles 100% After 10,000 cycles | [72] |
| Ti ₃ C ₂ T _x | PVA-H ₂ SO ₄ | 0 to 0.6 | 0.7–15 W cm ⁻³ | 11–18 mWh cm ⁻³ | 27 | 357 | 100% After 10,000 cycles | [66] |
| 3DMXene-r-GO composite aerogel | PVA-H ₂ SO ₄ | 0 to 0.6 | 180 μW cm ⁻² 60 μW cm ⁻² | 1.33 μWh cm ⁻² 2.18 μWh cm ⁻² | 34.6 | — | 15,000(91%) | [77] |
| MXene/BC composite paper electrodes | PVA-H ₂ SO ₄ | 0 to 0.6 | — | 0.00552 mWh cm ⁻² | 111.5 | — | 5000 (72.2%) | [76] |

| MSC | Electrolyte | Voltage window (V) | Device performance | | Specific capacitance | | Cycling stability | Ref |
|---|--|--------------------|----------------------------|---------------------------|---------------------------|--------------------------------|-------------------------|------|
| | | | Power density | Energy density | Areal/mF cm ⁻² | Volumetric/ F cm ⁻³ | | |
| Ti ₃ C ₂ T _x @Silver-plated Nylon Fiber Electrodes | PVA-H ₂ SO ₄ | 0 to 0.4 | 132 μW cm ⁻² | 73 μWh cm ⁻² | 328 | — | 10,000(80%) | [81] |
| r-GO/MnO ₂ /Ag NW-PET | SiO ₂ -1-butyl-3-methylimidazolium bis(trifluoromethylsulfonyl) imide | 0 to 2.5 | 162.0 mW. cm ⁻³ | 2.3 mWh. cm ⁻³ | — | 2.72 | 90.3% After 6000 cycles | [82] |
| VN// Co(OH) ₂ | KOH/PVA | 0 to 1.6 | 1750 mW cm ⁻³ | 12.4 mWh cm ⁻³ | 21 | 39.7 | 84% After 10,000 cycles | [83] |
| LSG/Ni-Catecholate-MOF | LiCl/PVA | 0 to 1.6 | 7 mWcm ⁻² | 4.1 Wh cm ⁻² | 15.2 | — | 87% After 5000 cycles | [84] |
| Asymmetric system | | | | | | | | |
| FGO//FrGO | PVA/Na ₂ SO ₄ | | 28.3 μW cm ⁻² | 2.52 μWh cm ⁻² | 73 | — | 100% over 500 cycles | [34] |
| MXene// MXene-MoO ₂ -AMSCs | PVA-H ₃ PO ₄ | 0 to 1.2 | 0.8 W cm ⁻³ | 9.7 mWh cm ⁻³ | 19 | 63.3 | 88% After 10,000 cycles | [85] |
| Co(OH) ₂ //erGO | PVA-KOH-KI | 0 to 1.4 | 100.38μWh cm ⁻² | 0.35μWh cm ⁻² | 2.28 | — | 89% After 10,000 cycles | [86] |

Table 3. Summary of recently reported all-solid-state MSCs based on 2D materials.

Recently, research has been put into the fabrication of 2D TMOs/TMHs for MSC electrodes, limitations remain when using electrode based on a single material. The major disadvantages mainly rely on poor rate capacity caused by low electrical conductivity, restricted enhancement of energy density, and low capacitance, limiting their practical implementations [87]. To surpass the challenges of using single electrode materials, it is appropriate to fabricate nanoarchitectures based on composites of TMOs/TMHs. This can hone the configuration to avoid the agglomeration of 2D nanosheets and raise the performance level of various electrode materials to execute effective enhancement of supercapacitor performance [89]. Inspired from these findings, Wang *et al.* developed all-solid-state planar asymmetric MSCs based on $\text{Co}(\text{OH})_2/\text{EG}$ and porous VN nanosheets/EG as positive and negative electrodes, respectively, together with an interdigital mask placed on the Nylon membrane. The developed electrodes showed high electrical conductivity, high flexibility, and homogeneity over a large area and were acted as flexible electrodes without any need for binder, additives and metal-constituted current collectors for VN// $\text{Co}(\text{OH})_2$ -PHMSs. The outstanding performance of the electrode was benefited from planar device geometry, synergy of $\text{Co}(\text{OH})_2$ nanoflower (charge storing like battery) and VN nanosheets (charging storing like capacitor) based hybrid structure, and highly conducting EG nanosheets, which served as both additives and current collectors. The enhancement of capacitance in PHMss (planar hybrid MSCs) was occurred due to the porous structure of VN and nanoflower morphology of $\text{Co}(\text{OH})_2$, these factors are suitable to enhance electrolyte ions and lessen their diffusion paths. The interdigital planar geometry of VN// $\text{Co}(\text{OH})_2$ -PHMSs permits the ultra-fast flow of electrolyte ions between the adjacent finger electrodes with a concise diffusion pathway. This improved charge storage via the effective exploration of highly active surface area of 2D nanosheets. Consequently, the fabricated PHMss exhibited areal capacitance of 21 mF cm^{-2} and volumetric capacitance of 39.7 F cm^{-3} with a notable energy density of 12.4 mWh cm^{-3} and 84% capacitance retention over 10,000 cycles [83]. Recently, Lee *et al.* fabricated an in-plane MSCs comprised of $\text{Co}(\text{OH})_2$ and r-GO through a cost-effective two-step fabrication method (**Figure 8a**). This method contained the fabrication of $\text{Co}(\text{OH})_2$ and r-GO on Au electrode using photolithography and electrodeposition method. The Au metal situated at the bottom of the electrode act as a current collector and effectively transfers electrons to the active material because of its high conductivity. The electrode's large surface area promotes the reaction between the electrolyte and the active material. This electrode structure maximizes the volumetric and areal capacitance of fabricated $\text{Co}(\text{OH})_2/\text{r-GO}$ ASC (**Figure 8b**), shows a power density of $100.38 \mu\text{W cm}^{-2}$ and energy density of $0.35 \mu\text{Wh cm}^{-2}$ for practical devices. and an excellent cycling capability with a capacitance retention up to 89% over 10,000 cycles, together with exceptional flexibility [86]. 2D MOFs are important 2D materials with tunable functionality and a designable porous structure with periodicity [90–92]. The high porosity of organic framework materials is suitable for producing electric double-layer capacitance and the heteroatoms like B, N, O and S located on the organic frameworks may show redox behavior for the pseudocapacitance [93]. The shortage of feasible microfabrication methods limits the practical implementation of MOF based electrode materials in MSCs. For the first time, a flexible symmetric MSC based on conductive Ni-catecholate-MOF possessing redox chemistry and high conductivity in the negative and positive windows was grown on 3D laser scribed graphene by Wu *et al.* The developed LSG/Ni-MOF-based MSCs showed outstanding areal capacitance of 15.2 mF cm^{-2} at 0.2 mA cm^{-2} . The π conjugation of tricatecholate ligands resulted in decent electrical conductivity. The flow of electrolytes is enhanced due to the porous 1D open channels formed by the alternative stacking of 2D layers. The fabricated MSCs displayed the

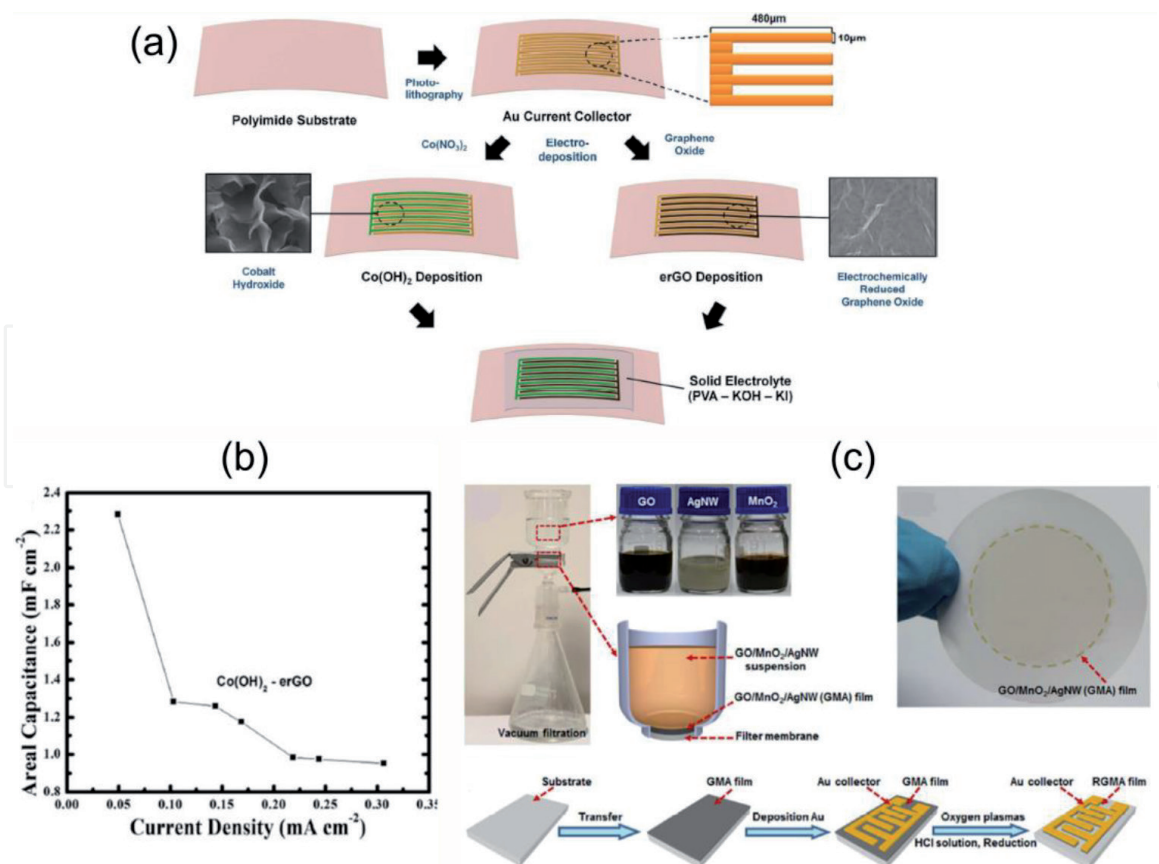


Figure 8.

(a) Schematic representation of the fabrication of Co(OH)₂-e-rGO, (b) the variation in areal capacitances v/s current density of Co(OH)₂/e-rGO MSC (Source: Reprinted from [13], with permission from RSC) and (c) schematic diagram of the fabrication of ternary hybrid film and displaying ternary hybrid film supported on cellulose acetate via vacuum filtration and fabrication process of RGO/MnO₂/Ag NW-MSCs on alumina (Source: Reprinted from [82], with permission from, copyright@2015, ACS).

highest power density of 7 mW cm⁻² and a high energy density of 4.1 μW h cm⁻². As illustrated in fig, MOF based MSC retained 87% of its initial capacitance in gel electrolyte even after 5000 cycles. This approach may shed light on fabricating novel MOF-based MSCs and electrochemical devices [84]. Recently, Liu *et al.* presented all-solid-state MSCs based on a flexible ternary hybrid film (RGMA) of RGO/MnO₂/AgNW (silver nanowire) via facile vacuum filtration and thermal reduction (Figure 8c). It provided a great advantage to include metal oxide or metal nanoarchitectures into graphene film with strong potential for various thin-film energy storage devices. They adopted an efficient strategy to design graphene-based nanoarchitectures by incorporating the high electrical conductivity, interface integrity of the components and energy storage mechanisms (pseudocapacitance and electric double layer capacitance). Graphene is good material for the flexible energy storage devices due to its mechanical stability and MnO₂ served to enhance the capacitive performances and inhibited the aggregation of graphene nanosheets. The ternary hybrid film's mechanical flexibility and electrical conductivity could be enhanced by the 1D AgNW, which functioned as a conducting bridge between Needle-like MnO₂ and graphene nanosheets. This flexible MSC delivers a specific capacitance of 2.72 F cm⁻³ and an excellent cycling capability with a capacitance retention up to 90.3% after 6000 cycles, together with exceptional flexibility and volumetric energy density of 2.3 mWh cm⁻³ (power density of 162.0 mW cm⁻³) in ionic liquid gel electrolyte [82]. Figure 9 illustrates the schematic representation of fabrication and characterization of all-solid-state MSCs based on 2D materials.

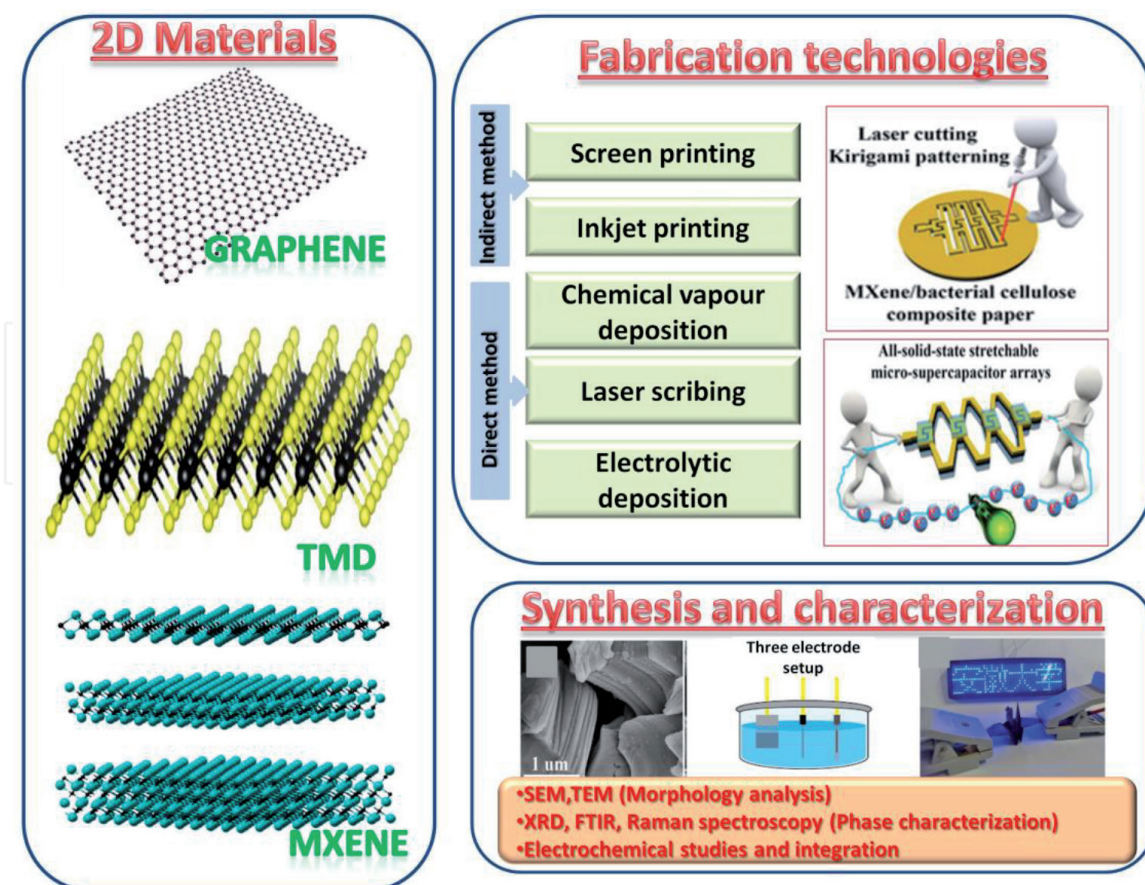


Figure 9. Schematic of fabrication and characterization of MSC based on 2D materials. Graphene structure (Mary, 2020), TMD structure (Wikipedia contributors. (2020, October 12). Transition metal dichalcogenide monolayers. In Wikipedia, The Free Encyclopedia. Retrieved 07:20, October 17, 2020, from https://en.wikipedia.org/w/index.php?title=Transition_metal_dichalcogenide_monolayers&oldid=983161701) MXene structure (Yujuan Zhang, Ningning Zhang and Changchun Ge- First-Principles Studies of Adsorptive Remediation of Water and Air Pollutants Using Two-Dimensional MXene Material, materials 2018, 11 [11], 2281. Three electrode setup (Benjamin Hsia- Materials Synthesis and Characterization for Micro-supercapacitor Applications, Doctoral dissertation, University of California, Berkeley (2013)). Fabrication technologies and Synthesis/characterization (Source: Reprinted from [76]).

5. Conclusion

MSCs as an energy storage devices attract considerable attention due to their notable characteristics such as smaller volume and high electrochemical performance. This chapter provides a brief overview of the recent developments in the field of 2D material-based all-solid-state MSCs. A brief note on the MSC device configuration and microfabrication methods for the microelectrodes has been illustrated. 2D materials based MSCs open up new avenues for the technologically relevant real-world applications. 2D materials such as MXenes, graphene, TMDs, and 2D metal–organic framework, TMOs/TMHs materials, have been described with regard to their electrochemical properties for MSCs. It is reported that the one issue faced by 2D materials is their unavoidable aggregation or restacking owing to their intense van der Waals interactions. To overcome this, there are approaches available like expansion of interlayer space with regard to enhanced storage ability or intercalation of guest molecules to increase the active sites. Moreover, for MSCs, 2D materials with vertical orientation grown on interdigitated current collectors is favorable to attain enhanced charge transport and low interfacial resistance. Additionally, to achieve higher conductivity and large specific surface area,

combining various materials with 2D hybrids is a practical approach to surpass each component material's challenges. Precisely, novel 2D materials with fascinating electrochemical properties are highly required. For example, 2D materials such as borophene, tellurene, silicene, phosphorene and germanene with higher electrical conductivity and enhanced specific surface area can be suitable candidates for high-performance MSCs. However, the coatings or surface functionalization of these 2D materials will be needed due to their chemical degradation and intrinsic surface instability under surrounding conditions. Above all, the processibility, reliability, and scalability of high-quality 2D materials are necessary not only for basic research but also for the real-world technological applications that need improved microfabrication methods such as screen printing and inkjet printing and 3D printing, *etc.*

Despite the recent advances in the design and fabrication of MSCs, MSC is still imperfect and require more developments. Some challenges limit practical implementation such as sustaining stable output voltage for wearable devices (microsystem and MSCs array just ignore these issues), current and output voltage are yet not pleased and more attempts should be assigned to design MSCs with a wider potential window. Moreover, various features, such as self-healing, hydrophobia, and stretchability, could be more developed to improve MSC performance. The device fabrication holds a significant role in technological innovation that, successively, affects the large scale production and the complexity of MSCs. It is expected that the integration of microdevices and smart functions into systems is unavoidable for facilitating the fast growth of smart electronic devices. MSCs based on 2D materials are focused on the powering of energy-consuming microdevices. Because of the complication in the smart systems' fabrication process, only limited works have been reported. So, innovative self-powered smart systems, including energy storage units, constitute a highly emerging research direction. Besides, the fabrication of a smart system with flexible, biodegradable and washable features can open the way for future independent, continuous, and intelligent daily electronics functioning. Moreover, these all-in-one self-powered systems can be used for health care applications in the future.

Acknowledgements

This work was financially supported by the Department of Science and Technology (DST)-SERB Early Career Research project (Grant No. ECR/2017/001850), DST-Nanomission (DST/NM/NT/2019/205(G), DST/TDT/SHRI-34/2018), Karnataka Science and Technology Promotion Society (KSTePS/VGST-RGS-F/2018-2019/GRD NO. 829/315).

Conflict of interest

The authors declare no conflict of interest.

IntechOpen

IntechOpen

Author details

Minu Mathew, Sithara Radhakrishnan and Chandra Sekhar Rout*
Centre for Nano and Material Sciences, Jain University, Jain Global Campus,
Jakkasandra, Ramanagaram, Bangalore, India

*Address all correspondence to: r.chandrasekhar@jainuniversity.ac.in;
csrout@gmail.com

IntechOpen

© 2020 The Author(s). Licensee IntechOpen. This chapter is distributed under the terms of the Creative Commons Attribution License (<http://creativecommons.org/licenses/by/3.0>), which permits unrestricted use, distribution, and reproduction in any medium, provided the original work is properly cited. 

References

- [1] Wang J, Li F, Zhu F, Schmidt OG. Recent Progress in Micro-Supercapacitor Design, Integration, and Functionalization. *Small Methods*. 2019;3(8): 1800367.
- [2] Zhang P, Wang F, Yu M, Zhuang X, Feng X. Two-dimensional materials for miniaturized energy storage devices: from individual devices to smart integrated systems. *Chem Soc Rev*. 2018;47(19):7426-51.
- [3] Yue Y, Liu N, Ma Y, Wang S, Liu W, Luo C, et al. Highly Self-Healable 3D Microsupercapacitor with MXene-Graphene Composite Aerogel. *ACS Nano*. 2018 May 22;12(5):4224-32.
- [4] Liu L, Zhao H, Lei Y. Advances on three-dimensional electrodes for micro-supercapacitors: A mini-review. *InfoMat*. 2019 Mar;1(1):74-84.
- [5] Feng X, Ning J, Wang D, Zhang J, Dong J, Zhang C, et al. All-solid-state planar micro-supercapacitor based on graphene/NiOOH/Ni(OH)₂ via mask-free patterning strategy. *J Power Sources*. 2019 Apr;418:130-7.
- [6] Qi D, Liu Y, Liu Z, Zhang L, Chen X. Design of Architectures and Materials in In-Plane Micro-supercapacitors: Current Status and Future Challenges. *Adv Mater*. 2017 Feb;29(5):1602802.
- [7] Shahrokhian S, Naderi L, Mohammadi R. High-Performance Fiber-Shaped Flexible Asymmetric Micro-Supercapacitor Based on Ni(OH)₂ Nanoparticles-Decorated Porous Dendritic Ni-Cu Film/Cu Wire and RGO/Carbon Fiber Electrodes. :47.
- [8] Yu D, Qian Q, Wei L, Jiang W, Goh K, Wei J, et al. Emergence of fiber supercapacitors. *Chem Soc Rev*. 2015;44(3):647-62.
- [9] Qi et al. - 2017 - Design of Architectures and Materials in In-Plane. pdf.
- [10] Liu N, Gao Y. Recent Progress in Micro-Supercapacitors with In-Plane Interdigital Electrode Architecture. *Small*. 2017 Dec;13(45).
- [11] Beidaghi M, Gogotsi Y. Capacitive energy storage in micro-scale devices: recent advances in design and fabrication of micro-supercapacitors. *Energy Environ Sci*. 2014;7(3):867.
- [12] Sollami Delekta S, Adolfsson KH, Benyahia Erdal N, Hakkarainen M, Östling M, Li J. Fully inkjet printed ultrathin microsupercapacitors based on graphene electrodes and a nano-graphene oxide electrolyte. *Nanoscale*. 2019;11(21):10172-7.
- [13] Lee SC, Patil UM, Kim SJ, Ahn S, Kang S-W, Jun SC. All-solid-state flexible asymmetric micro supercapacitors based on cobalt hydroxide and reduced graphene oxide electrodes. *RSC Adv*. 2016;6(50):43844-54.
- [14] Recent advances in micro-supercapacitors - *Nanoscale* (RSC Publishing) [Internet]. [cited 2020 Sep 8]. Available from: <https://pubs.rsc.org/en/content/articlelanding/2019/nr/c9nr01090d#!divAbstract>
- [15] Qin J, Das P, Zheng S, Wu Z-S. A perspective on two-dimensional materials for planar micro-supercapacitors. *APL Mater*. 2019 Sep 1;7(9):090902.
- [16] Gogotsi Y, Simon P. True Performance Metrics in Electrochemical Energy Storage. *Science*. 2011 Nov 18;334(6058):917-8.
- [17] Liang J, Mondal AK, Wang D-W, Iacopi F. Graphene-Based Planar

Microsupercapacitors: Recent Advances and Future Challenges. *Adv Mater Technol.* 2019;4(1):1800200.

[18] Sci-Hub | 2D Materials Beyond Graphene for High-Performance Energy Storage Applications. *Advanced Energy Materials*, 6(23), 1600671 | 10.1002/aenm.201600671 [Internet]. [cited 2020 Sep 9]. Available from: <https://sci-hub.se/10.1002/aenm.201600671>

[19] Sci-Hub | Engineering 2D Architectures toward High-Performance Micro-Supercapacitors. *Advanced Materials*, 1802793 | 10.1002/adma.201802793 [Internet]. [cited 2020 Sep 9]. Available from: <https://sci-hub.se/https://doi.org/10.1002/adma.201802793>

[20] Liu C, Yu Z, Neff D, Zhamu A, Jang BZ. Graphene-Based Supercapacitor with an Ultrahigh Energy Density. *Nano Lett.* 2010 Dec 8;10(12):4863-8.

[21] Wu Z-S, Parvez K, Feng X, Müllen K. Graphene-based in-plane micro-supercapacitors with high power and energy densities. *Nat Commun.* 2013 Sep 17;4(1):2487.

[22] Xiong G, Meng C, Reifenberger RG, Irazoqui PP, Fisher TS. A Review of Graphene-Based Electrochemical Microsupercapacitors. *Electroanalysis.* 2014 Jan;26(1):30-51.

[23] Zhang G, Han Y, Shao C, Chen N, Sun G, Jin X, et al. Processing and manufacturing of graphene-based microsupercapacitors. *Mater Chem Front.* 2018 Sep 27;2(10):1750-64.

[24] Yao B, Chandrasekaran S, Zhang J, Xiao W, Qian F, Zhu C, et al. Efficient 3D Printed Pseudocapacitive Electrodes with Ultrahigh MnO₂ Loading. *Joule.* 2019 Feb 20;3(2):459-70.

[25] Yue Y, Yang Z, Liu N, Liu W, Zhang H, Ma Y, et al. A Flexible

Integrated System Containing a Microsupercapacitor, a Photodetector, and a Wireless Charging Coil. *ACS Nano.* 2016 Dec 27;10(12):11249-57.

[26] Peng Z, Ye R, Mann JA, Zakhidov D, Li Y, Smalley PR, et al. Flexible Boron-Doped Laser-Induced Graphene Microsupercapacitors. *ACS Nano.* 2015 Jun 23;9(6):5868-75.

[27] Zhou F, Huang H, Xiao C, Zheng S, Shi X, Qin J, et al. Electrochemically Scalable Production of Fluorine-Modified Graphene for Flexible and High-Energy Ionogel-Based Microsupercapacitors. *J Am Chem Soc.* 2018 Jul 5;140(26):8198-205.

[28] Wang Y, Zhang Y, Liu J, Wang G, Pu F, Ganesh A, et al. Boosting areal energy density of 3D printed all-solid-state flexible microsupercapacitors via tailoring graphene composition. *Energy Storage Mater.* 2020 Sep;30:412-9.

[29] Sollami Delekta S, Laurila M-M, Mäntysalo M, Li J. Drying-Mediated Self-Assembly of Graphene for Inkjet Printing of High-Rate Micro-supercapacitors. *Nano-Micro Lett.* 2020 Jan;12(1):40.

[30] Kletenik-Edelman O, Ploshnik E, Salant A, Shenhar R, Banin U, Rabani E. Drying-Mediated Hierarchical Self-Assembly of Nanoparticles: A Dynamical Coarse-Grained Approach. *J Phys Chem C.* 2008 Mar 1;112(12):4498-506.

[31] Van Toan N, Kim Tuoi TT, Li J, Inomata N, Ono T. Liquid and solid states on-chip micro-supercapacitors using silicon nanowire-graphene nanowall-pani electrode based on microfabrication technology. *Mater Res Bull.* 2020 Nov 1;131:110977.

[32] All-graphene-battery: bridging the gap between supercapacitors and lithium ion batteries | *Scientific Reports* [Internet]. [cited 2020 Sep 14].

Available from: <https://www.nature.com/articles/srep05278>

[33] Yang - 2016 - Graphene and the related conductive inks for flexi.pdf.

[34] Lu Y, Zheng Y, Zhang H, He X, Yang Q, Wu J. A high performance and flexible in-plane asymmetric micro-supercapacitor (MSC) fabricated with functional electrochemical-exfoliated graphene. *J Electroanal Chem.* 2020 Jun 1;866:114169.

[35] Lochmann S, Grothe J, Eckhardt K, Leistenschneider D, Borchardt L, Kaskel S. Nanoimprint lithography of nanoporous carbon materials for micro-supercapacitor architectures. *Nanoscale.* 2018 May 31;10(21):10109-15.

[36] Zhang C (John), Kremer MP, Seral-Ascaso A, Park S-H, McEvoy N, Anasori B, et al. Stamping of Flexible, Coplanar Micro-Supercapacitors Using MXene Inks. *Adv Funct Mater.* 2018;28(9):1705506.

[37] Hota MK, Jiang Q, Mashraei Y, Salama KN, Alshareef HN. Fractal Electrochemical Microsupercapacitors. *Adv Electron Mater.* 2017 Oct;3(10):1700185.

[38] Stamp-assisted flexible graphene-based micro-supercapacitors - ScienceDirect [Internet]. [cited 2020 Sep 15]. Available from: <https://www.sciencedirect.com/science/article/abs/pii/S0378775320304699>

[39] Wu Y, Zhang Y, Liu Y, Cui P, Chen S, Zhang Z, et al. Boosting the Electrochemical Performance of Graphene-Based On-Chip Micro-Supercapacitors by Regulating the Functional Groups. *ACS Appl Mater Interfaces.* 2020 Sep 14;acsami.0c11085.

[40] Liu F, Liu C, Li X, Zhang L, Zhao W, Zhang G. Graphene-Based Integrated Planar On-Chip Micro-Supercapacitors

with No Internal Connection. *Integr Ferroelectr.* 2020 Mar 23;206(1):96-104.

[41] Yang S, Jiang C, Wei S. Gas sensing in 2D materials. *Appl Phys Rev.* 2017 Jun;4(2):021304.

[42] Gravure printing of hybrid MoS₂@S-rGO interdigitated electrodes for flexible microsupercapacitors: *Applied Physics Letters: Vol 107, No 1* [Internet]. [cited 2020 Sep 16]. Available from: <https://aip.scitation.org/doi/10.1063/1.4926570>

[43] W Y, L H, X T, M Y, H Y, X L, et al. Carbon-MEMS-Based Alternating Stacked MoS₂@rGO-CNT Micro-Supercapacitor with High Capacitance and Energy Density. *Small Weinbergstr Ger* [Internet]. 2017 May 30 [cited 2020 Sep 15];13(26). Available from: <https://europemc.org/article/med/28558128>

[44] Haider WA, Tahir M, He L, Yang W, Minhas-khan A, Owusu KA, et al. Integration of VS₂ nanosheets into carbon for high energy density micro-supercapacitor. *J Alloys Compd.* 2020 May;823:151769.

[45] Py MA, Haering RR. Structural destabilization induced by lithium intercalation in MoS₂ and related compounds. *Can J Phys.* 1983 Jan 1;61(1):76-84.

[46] Xu C, Jiang L, Li X, Li C, Shao C, Zuo P, et al. Miniaturized high-performance metallic 1T-Phase MoS₂ micro-supercapacitors fabricated by temporally shaped femtosecond pulses. *Nano Energy.* 2020 Jan;67:104260.

[47] Chen Y, Zhu X, Yang D, Wangyang P, Zeng B, Sun H. A novel design of poly (3,4-ethylenedioxythiophene):poly (styrenesulfonate)/molybdenum disulfide/poly (3,4-ethylenedioxythiophene) nanocomposites for fabric micro-supercapacitors with favourable

performances. *Electrochimica Acta*. 2019 Mar;298:297-304.

[48] Li B, Liang X, Li G, Shao F, Xia T, Xu S, et al. Inkjet-Printed Ultrathin MoS₂-Based Electrodes for Flexible In-Plane Microsupercapacitors. *ACS Appl Mater Interfaces*. 2020 Sep 2;12(35):39444-54.

[49] El-Kady MF, Kaner RB. Scalable fabrication of high-power graphene micro-supercapacitors for flexible and on-chip energy storage. *Nat Commun*. 2013 Feb 12;4(1):1475.

[50] Wu Z-S, Parvez K, Feng X, Müllen K. Photolithographic fabrication of high-performance all-solid-state graphene-based planar micro-supercapacitors with different interdigital fingers. *J Mater Chem A*. 2014 May 15;2(22):8288-93.

[51] Gao W, Singh N, Song L, Liu Z, Reddy ALM, Ci L, et al. Direct laser writing of micro-supercapacitors on hydrated graphite oxide films. *Nat Nanotechnol*. 2011 Jul 31;6(8):496-500.

[52] Hsia B, Marschewski J, Wang S, In JB, Carraro C, Poulikakos D, et al. Highly flexible, all solid-state micro-supercapacitors from vertically aligned carbon nanotubes. *Nanotechnology*. 2014 Feb 7;25(5):055401.

[53] Kim SK, Koo HJ, Lee A, Braun PV. Selective wetting-induced micro-electrode patterning for flexible micro-supercapacitors. *Adv Mater*. 2014 Aug 13;26(30):5108-12.

[54] Huang P, Lethien C, Pinaud S, Brousse K, Laloo R, Turq V, et al. On-chip and freestanding elastic carbon films for micro-supercapacitors. *Science*. 2016 Feb 12;351(6274):691-5.

[55] Chmiola J, Largeot C, Taberna P-L, Simon P, Gogotsi Y. Monolithic carbide-derived carbon films for micro-supercapacitors. *Science*. 2010 Apr 23;328(5977):480-3.

[56] Beidaghi M, Wang C. Micro-Supercapacitors Based on Interdigital Electrodes of Reduced Graphene Oxide and Carbon Nanotube Composites with Ultrahigh Power Handling Performance. *Adv Funct Mater*. 2012;22(21):4501-10.

[57] Song B, Li L, Lin Z, Wu Z-K, Moon K, Wong C-P. Water-dispersible graphene/polyaniline composites for flexible micro-supercapacitors with high energy densities. *Nano Energy*. 2015 Sep 1;16:470-8.

[58] Kurra N, Jiang Q, Alshareef HN. A general strategy for the fabrication of high performance microsupercapacitors. *Nano Energy*. 2015 Sep 1;16:1-9.

[59] Kurra N, Alhebshi NA, Alshareef HN. Microfabricated Pseudocapacitors Using Ni(OH)₂ Electrodes Exhibit Remarkable Volumetric Capacitance and Energy Density. *Adv Energy Mater*. 2015;5(2):1401303.

[60] Si W, Yan C, Chen Y, Oswald S, Han L, Schmidt OG. On chip, all solid-state and flexible micro-supercapacitors with high performance based on MnOx/Au multilayers. *Energy Environ Sci*. 2013 Oct 18;6(11):3218-23.

[61] Tahir M, He L, Yang W, Hong X, Haider WA, Tang H, et al. Boosting the electrochemical performance and reliability of conducting polymer microelectrode via intermediate graphene for on-chip asymmetric micro-supercapacitor. *J Energy Chem*. 2020 Oct 1;49:224-32.

[62] Cao L, Yang S, Gao W, Liu Z, Gong Y, Ma L, et al. Direct Laser-Patterned Micro-Supercapacitors from Paintable MoS₂ Films. *Small*. 2013;9(17):2905-10.

[63] Beidaghi M, Gogotsi Y. Capacitive energy storage in micro-scale devices: recent advances in design and fabrication of micro-supercapacitors.

- Energy Environ Sci. 2014 Feb 20;7(3):867-84.
- [64] Acerce M, Voiry D, Chhowalla M. Metallic 1T phase MoS₂ nanosheets as supercapacitor electrode materials. *Nat Nanotechnol.* 2015 Apr;10(4):313-8.
- [65] Zhang P, Wang F, Yu M, Zhuang X, Feng X. Two-dimensional materials for miniaturized energy storage devices: from individual devices to smart integrated systems. *Chem Soc Rev.* 2018 Oct 1;47(19):7426-51.
- [66] Peng Y-Y, Akuzum B, Kurra N, Zhao M-Q, Alhabeab M, Anasori B, et al. All-MXene (2D titanium carbide) solid-state microsupercapacitors for on-chip energy storage. *Energy Environ Sci.* 2016 Aug 31;9(9):2847-54.
- [67] Dillon AD, Ghidiu MJ, Krick AL, Griggs J, May SJ, Gogotsi Y, et al. Highly Conductive Optical Quality Solution-Processed Films of 2D Titanium Carbide. *Adv Funct Mater.* 2016;26(23):4162-8.
- [68] Naguib M, Mochalin VN, Barsoum MW, Gogotsi Y. Two-Dimensional Materials: 25th Anniversary Article: MXenes: A New Family of Two-Dimensional Materials (*Adv. Mater.* 7/2014). *Adv Mater.* 2014;26(7):982-982.
- [69] Ghidiu M, Lukatskaya MR, Zhao M-Q, Gogotsi Y, Barsoum MW. Conductive two-dimensional titanium carbide 'clay' with high volumetric capacitance. *Nature.* 2014 Dec;516(7529):78-81.
- [70] Ghidiu M, Lukatskaya MR, Zhao M-Q, Gogotsi Y, Barsoum MW. Conductive two-dimensional titanium carbide 'clay' with high volumetric capacitance. *Nature.* 2014 Dec;516(7529):78-81.
- [71] Yan J, Wang Q, Wei T, Jiang L, Zhang M, Jing X, et al. Template-assisted low temperature synthesis of functionalized graphene for ultrahigh volumetric performance supercapacitors. *ACS Nano.* 2014 May 27;8(5):4720-9.
- [72] Zhang C (John), McKeon L, Kremer MP, Park S-H, Ronan O, Seral-Ascaso A, et al. Additive-free MXene inks and direct printing of micro-supercapacitors. *Nat Commun.* 2019 Apr 17;10(1):1795.
- [73] Peng Y-Y, Akuzum B, Kurra N, Zhao M-Q, Alhabeab M, Anasori B, et al. All-MXene (2D titanium carbide) solid-state microsupercapacitors for on-chip energy storage. *Energy Environ Sci.* 2016 Aug 31;9(9):2847-54.
- [74] Huang H, Chu X, Su H, Zhang H, Xie Y, Deng W, et al. Massively manufactured paper-based all-solid-state flexible micro-supercapacitors with sprayable MXene conductive inks. *J Power Sources.* 2019 Mar 1;415:1-7.
- [75] Zhang H, Cao Y, Chee MOL, Dong P, Ye M, Shen J. Recent advances in micro-supercapacitors. *Nanoscale.* 2019 Mar 28;11(13):5807-21.
- [76] Jiao S, Zhou A, Wu M, Hu H. Kirigami Patterning of MXene/Bacterial Cellulose Composite Paper for All-Solid-State Stretchable Micro-Supercapacitor Arrays. *Adv Sci.* 2019;6(12):1900529.
- [77] Yue Y, Liu N, Ma Y, Wang S, Liu W, Luo C, et al. Highly Self-Healable 3D Microsupercapacitor with MXene-Graphene Composite Aerogel. *ACS Nano.* 2018 May 22;12(5):4224-32.
- [78] Li P, Shi W, Liu W, Chen Y, Xu X, Ye S, et al. Fabrication of high-performance MXene-based all-solid-state flexible microsupercapacitor based on a facile scratch method. *Nanotechnology.* 2018 Sep;29(44):445401.
- [79] Jiang Q, Wu C, Wang Z, Wang AC, He J-H, Wang ZL, et al. MXene

electrochemical microsupercapacitor integrated with triboelectric nanogenerator as a wearable self-charging power unit. *Nano Energy*. 2018 Mar 1;45:266-72.

[80] Xu S, Liu W, Liu X A MXene based all-solid-state microsupercapacitor with 3D interdigital electrode, 19th international conference on solid state sensors, Actuators and Sensors. 2017 Jun 18;706-709.

[81] Hu M, Li Z, Li G, Hu T, Zhang C, Wang X. All-Solid-State Flexible Fiber-Based MXene Supercapacitors. *Adv Mater Technol*. 2017;2(10):1700143.

[82] Liu W, Lu C, Wang X, Tay RY, Tay BK. High-Performance Microsupercapacitors Based on Two-Dimensional Graphene/Manganese Dioxide/Silver Nanowire Ternary Hybrid Film. *ACS Nano*. 2015 Feb 24;9(2):1528-42.

[83] Wang S, Wu Z-S, Zhou F, Shi X, Zheng S, Qin J, et al. All-solid-state high-energy planar hybrid micro-supercapacitors based on 2D VN nanosheets and Co(OH)₂ nanoflowers. *Npj 2D Mater Appl*. 2018 Mar 26;2(1):1-8.

[84] Wu H, Zhang W, Kandambeth S, Shekhah O, Eddaoudi M, Alshareef HN. Conductive Metal–Organic Frameworks Selectively Grown on Laser-Scribed Graphene for Electrochemical Microsupercapacitors. *Adv Energy Mater*. 2019;9(21):1900482.

[85] Zhang L, Yang G, Chen Z, Liu D, Wang J, Qian Y, et al. MXene coupled with molybdenum dioxide nanoparticles as 2D-0D pseudocapacitive electrode for high performance flexible asymmetric micro-supercapacitors. *J Materiomics*. 2020 Mar 1;6(1):138-44.

[86] Lee SC, Patil UM, Kim SJ, Ahn S, Kang S-W, Jun SC. All-solid-state flexible

asymmetric micro supercapacitors based on cobalt hydroxide and reduced graphene oxide electrodes. *RSC Adv*. 2016 May 3;6(50):43844-54.

[87] Jiang J, Li Y, Liu J, Huang X, Yuan C, Lou XWD. Recent advances in metal oxide-based electrode architecture design for electrochemical energy storage. *Adv Mater Deerfield Beach Fla*. 2012 Oct 2;24(38):5166-80.

[88] Gao S, Sun Y, Lei F, Liang L, Liu J, Bi W, et al. Ultrahigh Energy Density Realized by a Single-Layer β -Co(OH)₂ All-Solid-State Asymmetric Supercapacitor. *Angew Chem Int Ed*. 2014;53(47):12789-93.

[89] Guan M, Wang Q, Zhang X, Bao J, Gong X, Liu Y. Two-Dimensional Transition Metal Oxide and Hydroxide-Based Hierarchical Architectures for Advanced Supercapacitor Materials. *Front Chem [Internet]*. 2020 [cited 2020 Sep 19];8. Available from: <https://www.frontiersin.org/articles/10.3389/fchem.2020.00390/full>

[90] Dang S, Zhu Q-L, Xu Q. Nanomaterials derived from metal–organic frameworks. *Nat Rev Mater*. 2017 Dec 5;3(1):1-14.

[91] Mandal AK, Mahmood J, Baek J-B. Two-Dimensional Covalent Organic Frameworks for Optoelectronics and Energy Storage. *ChemNanoMat*. 2017;3(6):373-91.

[92] Liu J, Wöll C. Surface-supported metal–organic framework thin films: fabrication methods, applications, and challenges. *Chem Soc Rev*. 2017 Oct 2;46(19):5730-70.

[93] Zhang P, Wang F, Yu M, Zhuang X, Feng X. Two-dimensional materials for miniaturized energy storage devices: from individual devices to smart integrated systems. *Chem Soc Rev*. 2018 Oct 1;47(19):7426-51.